https://doi.org/10.5194/egusphere-2024-1226
Preprint. Discussion started: 1 July 2024

CO_2 flux characteristics of the grassland ecosystem and its response to environmental factors in the dry-hot valley of Jinsha River, China

Chaolei Yang[a,b,c,d], Yufeng Tian[a,b,c,d,*], Jingqi Cui[e], Guangxiong He[f], Jingyuan Li[e], Canfeng Li[a,b,c], Haichuang Duan[a], Zong Wei[a,b], Liu Yan[a,b] , Xin Xia[a,b] ,Yong Huang[a,b], Aihua Jiang[a,b]

[a] Kunming General Survey of Natural Resources Center, China Geological Survey, Kunming, 650111, China
[b] Yunnan Province Field Science Observation and Research Station on the Evolution of Soil and Water Resources and the Carbon Sequestration Enhancement Effects in the Alpine Gorge Area of the Jinsha River, Chuxiong, 651400, China
[c] Technology Innovation Center for Natural Carbon Sink, Kunming, 650111, China
[d] Key Laboratory of Coupling Process and Effect of Natural Resources Elements, Beijing, 100055, China
[e] Institute of Space Weather, School of Atmospheric Physics, Nanjing University of Information Science and Technology, Nanjing, 210044, China
[f] Tropical Eco-Agriculture Research Institute, Yunnan Academy of Agricultural Sciences, Chuxiong, 651300, China

Correspondence to: Yufeng Tian (yufeng_tian818@126.com)

ABSTRACT: The dry-hot valley of Jinsha River is distinguished by prolonged drought and high temperatures, making it a distinct non-zonal hot island habitat in the global temperate zone. It is an ideal location for studying changes in plant carbon budget under sustained drought and high-temperature conditions. However, there is currently a dearth of reports on CO_2 flux variations within plant ecosystems in this region. The study quantitatively analyzed the characteristics of CO_2 flux variation in the grassland ecosystem in this region and its response mechanisms to environmental factors using continuous observation data obtained from static assimilative chamber. The results indicate that both the environmental factors and CO_2 flux variations in grassland ecosystems exhibit significant seasonal characteristics. During the dry season (March to May), the grassland acts as a carbon source, exhibiting a daily average CO_2 flux of 0.1632 $\mu mol \cdot m^{-2} \cdot s^{-1}$, which cumulative CO_2 emissions for each month were 18.64 $g \cdot m^{-2}$, 15.96 $g \cdot m^{-2}$, and 20.64 $g \cdot m^{-2}$, respectively. The ecosystem showed noteworthy carbon absorption characteristics during the rainy season (August to October), with a daily average CO_2 flux of −0.1062 $\mu mol \cdot m^{-2} \cdot s^{-1}$, which cumulative CO_2 absorption for each month were 6.42 $g \cdot m^{-2}$, 24.41 $g \cdot m^{-2}$, and 5.14 $g \cdot m^{-2}$, respectively. Throughout the year, the ecosystem was a weak carbon source, emitting an annual cumulative CO_2 of 0.7078 $t \cdot ha^{-1} \cdot a^{-1}$, demonstrating carbon-neutral traits. In terms of environmental factors, there was a robust negative correlation exists with CO_2 flux between photosynthetically active radiation during the rainy season ($R = -0.578$, $P<0.01$). The daily CO_2 flux in different seasons was positively correlated with precipitation and relative humidity ($P<0.01$), and negatively correlated with air temperature, soil

https://doi.org/10.5194/egusphere-2024-1226
Preprint. Discussion started: 1 July 2024

temperature and vapor pressure deficit (P<0.01). The diurnal variation of CO_2 flux in dry season was mainly affected by relative humidity, while that in rainy season was mainly affected by relative humidity and vapor pressure deficit. The variation of CO_2 flux was most influenced by soil water content, relative humidity, and vapor pressure deficit at both daily and monthly scales throughout the year. The influence of temperature factor on CO_2 flux changes at different time scales is generally weak.

Key words: dry-hot valley of Jinsha River; savanna; grassland ecosystem; CO_2 flux; environmental factors

1 Introduction

Since the industrial revolution, human economic and social progress heavily relies on fossil energy consumption, the excessive release of greenhouse gases has resulted in a rise in atmospheric CO_2 concentration and climate warming (Sha et al., 2022; Wang et al., 2023), and has also produced a series of ecological and environmental problems. The terrestrial ecosystem can absorb about 15.0%–30.0% of anthropogenic CO_2 emissions per year and carbon-neutrality-capacity index reach 27.14% (Green et al., 2019; Bai et al., 2023; Liu et al., 2023; Zeng et al., 2023), which is a significant carbon sink (Piao et al., 2018; Yang et al., 2022), studying the dynamic shifts in the carbon budget and carbon-neutrality-capacity within global terrestrial ecosystems, along with their environmental driving factors, has emerged as a significant topic in the realm of global change (Houghton, 2001; Bai et al., 2023). Constituting about 40.5% of the global land surface, grasslands serve as a crucial element of terrestrial ecosystems, and its carbon storage represents around 1/3 of the total terrestrial carbon storage globally, equivalent to the carbon storage of forest ecosystems (White et al., 2000; Wang et al., 2021; Bai et al., 2022), in which organic carbon storage is about 525 Pg C (1Pg=10^{15} g) (Fang et al., 2007; Bai et al., 2022), significantly influencing the global carbon balance.

The savanna ecosystems cover 1/6 of the Earth’s total land area (Grace et al., 2006), which ecosystem structure and vegetation community composition are significantly controlled by hydrological conditions (Yu et al., 2015; Lee et al., 2018; Jin et al., 2019; Zhang et al., 2019; Hoffmann, 2023) and are composed of mixed forest and grassland ecosystems. The vegetation is mainly composed of grass, with sparse distribution of trees and shrubs. Being a significant component of the worldwide grassland ecosystem, and its net primary productivity (NPP) is about 30.0% of the terrestrial ecosystems (Grace et al., 2006; Peel et al., 2007; Dobson et al., 2022), which has significant impacts on global material cycling, energy flow, and climate change. Related

https://doi.org/10.5194/egusphere-2024-1226
Preprint. Discussion started: 1 July 2024

researches have indicated that the herbaceous plants in the savanna ecosystem are mainly C_4 grasses, but only have medium productivity, and their carbon flux changes are highly seasonal (Grace et al., 2006). The rainy season is mainly dominated by carbon absorption, and the maximum rate of carbon fixation can reach 2/3 of the maximum value of the tropical rainforest. The dry season is marked by weak carbon emission or weak carbon sinks (Grace et al., 1995; Malhi., 1998; Saleska et al., 2003; Bousquet et al., 2006; Millard et al., 2008; Livesley et al., 2011; Fei et al., 2017a). Furthermore, in the tropical savanna ecosystem, grass-derived carbon contributes to over half of the total soil organic carbon in the soil up to a depth of 1 meter, even in the soil under the tree, that is, the carbon in the soil mainly comes from herbaceous plants (Zhou et al., 2023). Simultaneously, ince the savanna ecosystem mainly stores carbon in the soil rather than the biomass of trees, certain researchers have suggested that it may emerge as a more significant carbon sink resource than forests in the future (Dobson et al., 2022).

The savanna ecosystem in China is mainly manifested as the ecological landscape of the valley-type sparsely shrub-grass vegetation distributed in the special geographical unit of the dry-hot valley, which is similar to the tropical savanna grassland. It is also known as valley-type savanna vegetation or semi-savanna vegetation (Jin et al., 1987; Shen et al., 2010). It is mainly distributed occurs in the Yuanjiang (YJ), Nu River, and Jinsha River (JS), and their tributaries in southwest China. The ecosystem is characterized by extremely high annual average temperature and lack of water source. The species richness increases with altitude (He et al., 2024), which belongs to the non-regional high temperature arid area evolved from the global temperate humid climate zone (Zhang, 1992). At present, there are limited studies on the carbon balance of the savanna ecosystem in the dry-hot valley of China. The existing studies primarily concentrate on the YJ. In the investigation of soil respiration dynamics in the savanna ecosystem of the YJ, Yang et al. (2020) discovered that the annual total carbon emission from soil respiration in this region is relatively low compared to global savanna ecosystems, at 4.20 $t \cdot ha^{-1} \cdot a^{-1}$. Fei et al. (2017a) revealed that the savanna ecosystem of the YJ was a carbon sink, and about 84.0% of the carbon sinks was mainly concentrated in the rainy season (1.08 ± 0.35 t C ha^{-1}), and the dry season was carbon neutral. With the backdrop of forthcoming climate change by rising temperatures and diminished rainfall, the ecosystem's carbon sink capacity could potentially decrease. The dry-hot valley of JS is the largest dry-hot valley in China, and it is also a typical representative of the valley-type savanna ecosystem in China. However, monitor and research on the CO_2 flux (*Fc*) features in this region is still lacking.

The research focused on the grassland ecosystem in the dry-hot valley of JS, utilizing actual observation data obtained by the static assimilative box method to explore the characteristics and

https://doi.org/10.5194/egusphere-2024-1226
Preprint. Discussion started: 1 July 2024

changes of the F*c* in ecosystem, and its correlation with related environmental factors, and calculate the annual F*c* of the ecosystem. In order to offer a scientific reference for in-depth comprehension of the key processes of carbon cycle in the valley-type savanna in China, and to study and predict the ecological function changes of vegetation carbon sequestration under continuous drought and high temperature stress in the future.

2 Data and methods

2.1 Observation sites

All observational data were derived from the Jinsha River Field Observation Station (26°4'6.24" N, 101°49'41.68" E), whose test site is situated in the Shikanzi Daqing River Basin on the west bank of JS (Fig. 1), with a representative savanna ecological landscape. The elevation of the basin is 1200–1800 m, falling within the realm of the southern subtropical dry-hot monsoon climate, with the characteristics of drought, high temperature and less rain. The ecosystem is extremely fragile and sensitive. The annual average temperature is 22.93°C, with daily maximum temperatures reaching over 43.00°C. The region has distinct rainy season (June to October) and dry season (November to May of the subsequent year), and the annual precipitation is 428.50 mm, with over 90.0% of the precipitation concentrated in the rainy season. The annual evaporation rate is high, typically 3–6 times the annual precipitation (He et al., 2000). Herbaceous plants are mainly *Heteropogon contortus* (Linn.) Beauv., *Eulaliopsis binate* (Retz.) C. E. Hubb, *Cymbopogon goeringii* (Steud.) A. Camus, *Eulalia specios*a (Debeaux) Kuntze, and so on. The shrubs include *Phyllanthus emblica* L., *Pistacia weinmannifolia* J. Poisson ex Franch, *Quercus franchetii* Skan, *Quercus cocciferoides* Hand. –Mazzz, *Dodonaea viscosa* (L.) Jacq., *Albizia kalkora* (Roxb.) Prain, *Osteomeles schwerinae* Schneid., *Osyris wightiana*, and *Terminalia franchetii* Gagnep. , etc.

2.2 Data source

2.2.1 Micrometeorological Factor Observation

The micro-meteorological factors were continuously monitored in real-time by the DL3000 small automatic meteorological observation system deployed in the test site of the observation station. The observation time began on January 12, 2023, and the observation indexes included air temperature (Ta), relative humidity (RH), soil temperature (Ts), soil water content (SWC), soil conductivity (SC), precipitation (P), wind speed (Ws), wind direction (WD), and photosynthetically active radiation (PAR). The average value of the environmental factors observation data for 5 minutes, 30 minutes, and 24 hourh are automatically recorded through the CR1000X data collector. The specific meteorological observation system sensor equipment information is listed in Table 1.

https://doi.org/10.5194/egusphere-2024-1226
Preprint. Discussion started: 1 July 2024

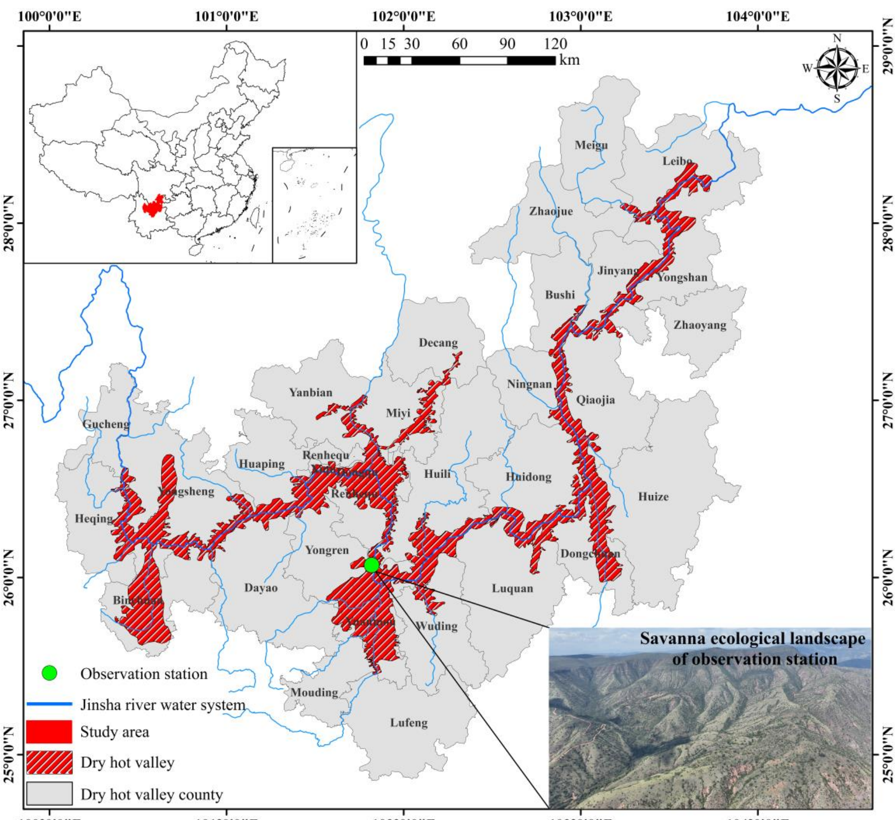

Figure 1 Range of dry-hot valley in JS and location of the Jinsha River Field Observation Station.

Table 1 Information of micrometeorological observation system.

Name of instrument	Observation parameter	Height (depth) of installation (m)
Temperature and humidity sensor	Ta (°C) and RH (%)	1.5
Photosynthetic effective radiometer	PAR (μmol·m^{-2}·s^{-1})	1.5
Wind speed and direction sensor	Ws (m/s) and WD (°)	1.5
Rainfall sensor	P (mm)	1.5
Soil multi-parameter sensor	Ts (°C), SWC (m^3 • m^{-3}), and SC (dS/m)	Soil horizon 0.1

2.2.2 CO_2 flux observation

In order to ensure the representativeness of the observation plots and the spatial integration of the observation data, the typical grassland plots with small micro-habitat differences were selected in the test site of the observation station to lay out and install static assimilative boxes for positioning observation. The observation point is about 10 m away from the automatic meteorological observation system. The observation time begins at 15:05 noon on March 3, 2023, and ends at 10:50

https://doi.org/10.5194/egusphere-2024-1226
Preprint. Discussion started: 1 July 2024

a.m. on November 1, 2023. The bottom area of the assimilative box is 0.25 m^2, and the volume in the box is 125 L. The whole box is composed of transparent organic glass. There are two sets of fans in the box, which can fully mix the gas evenly. The height of the base is 8cm, embedded in the underground soil is 5 cm, and the aboveground part is 3 cm. The NEE is mainly measured by the CARBOCAP ® carbon dioxide sensor GMP343 of Visala Company. The diffusion probe of the sensor can effectively reduce the measurement error caused by the pressure difference of the pumping system. It has the characteristics of flexibility and high precision and is widely used in ecosystem CO_2 monitoring. The top cover of the assimilative box can be automatically opened and closed, and the time of a single complete measurement cycle is 15 minutes. Before the measurement, the top cover of the assimilative box will be automatically opened, so that the gas in the box and the surrounding air are mixed evenly, and the time is 5 minutes. Then the top cover of the box is automatically closed to a closed and stable state, the fan starts, and the gas change in the box is measured. The measurement and recording time is 10 minutes, so repeated.

2.2.3 Other data

The boundary data of dry-hot valley was sourced from Deng (2022). The administrative boundary data (Xu, 2023a; Xu, 2023b) and river data (Xu, 2018) were sourced from the Resources and Environment Science Data Center (RESDC) from the Chinese Academy of Sciences.

2.2.4 Data processing

When the carbon flux is measured, the whole monitoring system will collect the original data of GMP34 at a speed of 2 Hz through the CR1000X data collector, and make an average of 5 seconds (main scan interval) to participate in the statistics. If the difference between the newly acquired data and the average value exceeds 8 times the standard deviation, it is classified as an outlier, and such data points are eliminated. The system performs linear regression fitting on the removed data and calculates the ecosystem CO_2 exchange capacity, goodness of fit, etc.

The ecosystem CO_2 exchange capacity is calculated by the formula (1):

$$F_c = \frac{V \times P_{av} \times (1000 - W_{av})}{R \times S \times (T_{av} + 273)} \times \frac{\partial_c}{\partial_t} (1)$$

where F_c represents CO_2 flux (μmol·m^{-2}·s^{-1}); V represents the volume of assimilative chamber (m^3); P_{av} represents the mean atmospheric pressure (kPa) inside the chamber during the observation period; W_{av} represents the partial pressure of water vapor inside the chamber during the observation period (mmol·mol^{-1}); R represents the atmospheric constant (8.314 J·mol^{-1}·K^{-1}); S represents the area of assimilative chamber (m^2); ∂_c / ∂_t represents the diffusion rate of CO_2 in the chamber; T_{av} represents the mean temperature (°C) inside the chamber during the observation period.

The linear regression method was employed to fit the CO_2 diffusion rate (∂_c / ∂) (formula 2).

https://doi.org/10.5194/egusphere-2024-1226
Preprint. Discussion started: 1 July 2024

This method is the basic method for measuring the CO_2 diffusion rate of most soil respiration and is widely used (Wen et al., 2007):

$$c(t) = c + \frac{\partial_c}{\partial_t} t \quad (2)$$

where *c(t)* represents the CO_2 concentration within the assimilative chamber; *t* represents the determination time; *c* represents the CO_2 concentration in the assimilative chamber when it is closed.

Taking into account the specific conditions of the study area, the recorded F*c* data was categorized into dry season (March 3rd–May 31st) and rainy season (June 1st–November 1st). Due to the damage of the assimilative box from June 1st to August 6th and the lack of observation data, considering the continuity of the data time series and the precision of the data, the dry season carbon flux data is mainly based on the observation data from March 4th to May 31st, and the rainy season carbon flux data is mainly based on the observation data from August 7th to October 31st. Quality control was conducted on the raw data to remove invalid NAN values and abnormal data. Utilizing the research results from Zhao et al. (2020), missing data points with a time difference of under 3 hours are filled in using linear interpolation. For data with a missing time gap exceeding 3 hours, differentiate and interpolate the data based on different time intervals. Among them, the data of daytime in the rainy season were interpolated by formula (3) rectangular hyperbolic model (Ruimy et al., 1995) to simulate the relationship between NEE and PAR. The missing data of the rainy season at nighttime and the dry season were interpolated by the multiplicative model (4) of the response of ecosystem respiration to Ts and SWC:

$$NEE_{daytime} = R_{daytime} - \frac{A_{max} \times \alpha \times PAR_{daytime}}{A_{max} + \alpha \times PAR_{daytime}} (3)$$

where $NEE_{daytime}$ represents the NEE during the daytime (μmol·m^{-2}·s^{-1}); A_{max} represents the maximum photosynthetic rate (μmol·m^{-2}·s^{-1}); α represents the apparent quantum efficiency (μmol·mol^{-1}); $R_{daytime}$ represents the daytime ecosystem respiration rate (μmol·m^{-2}·s^{-1}); $PAR_{daytime}$ represents the PAR during the daytime (μmol·m^{-2}·s^{-1}).

$$ER = a \times e^{\beta T_s} \times SWC^{C} (4)$$

where *ER* represents the ecosystem respiration rate (μmol·m^{-2}·s^{-1}); α, β and *c* represents the fitting parameters; *Ts* and *SWC* are shown in Table 1.

The vapor pressure deficit (VPD) is calculated by formula (5) (Campbell et al., 2012):

$$VPD = 0.61078 e^{\frac{17.27Ta}{Ta+237.3}} (1 - RH) (5)$$

where *RH* and *Ta* are shown in Table 1.

https://doi.org/10.5194/egusphere-2024-1226
Preprint. Discussion started: 1 July 2024

3 Analysis of the effect

3.1 Dynamic changes in environmental factors

Utilizing the observational data of micrometeorological factors, the dynamic attributes of environmental factors such as Ta, VPD, RH, P, Ws, PAR, Ts and SWC. It can be seen that these environmental factors showed a high degree of seasonal characteristics, especially the P and SWC were the most obvious. Among them, the P in the rainy season was 400.80 mm, and mainly concentrated in August (142 mm), the precipitation frequency was 17 times, and the SWC changes between 0–0.19 $m^3·m^{-3}$, also showing a strong response relationship with P (Fig. 2a and 2b). The minimum RH was 20.65% and the maximum was 94.10%, showing a strong response relationship with P. The VPD fluctuates between 0.11–4.13 kPa, and its value decreases significantly after May, which was related to the increase of P and RH in the rainy season (Fig. 2a and 2c). During the observation period, the PAR varied from 52.28–860.59 $μmol·m^{-2}·s^{-1}$, influenced by weather conditions and displaying significant fluctuations (Fig. 2d). From different seasons, the daily average of PAR in the dry season (476.50 $μmol·m^{-2}·s^{-1}$) exceeded that of the rainy season (432.79 $μmol·m^{-2}·s^{-1}$). During the dry season, the mean Ta was 23.04°C, while in the rainy season, it averaged 25.38°C. The difference was small. Secondly, the highest and lowest values of Ta appear in May of the dry season. The range of Ta and Ts was 8–34.52°C and 11.58–36.97°C, respectively. The seasonal variation characteristics of the two were similar, but the Ts was significantly higher than the Ta, and the change time lags behind the Ta (Fig. 2e). In terms of changes in Ws characteristics, the highest value of Ws appeared in March, reaching 2.93 $m·s^{-1}$, and the lowest value appeared in June, which was 0.57 $m·s^{-1}$. The daily average Ws was the highest in February, which was 1.90 $m·s^{-1}$, and the lowest in August, which was 0.99 $m·s^{-1}$. The Ws decreased significantly after mid-July (Fig. 2f).

3.2 Diurnal variation of CO_2 flux

The F*c* was positive, showing a carbon emission state, throughout the entire diurnal variation process in the dry season. The diurnal variation showed a 'W'-type bimodal curve (Fig. 3a) of decreasing → increasing → decreasing → increasing, that is, the F*c* was lower in the morning and afternoon, and the F*c* was higher in the nighttime and noon, especially in April and May when this diurnal variation pattern was most pronounced. The lowest F*c* values appeared in the morning (8:00–10:00) of each month, which were 0.1178 $μmol·m^{-2}·s^{-1}$, 0.1148 $μmol·m^{-2}·s^{-1}$, and 0.1397 $μmol·m^{-2}·s^{-1}$, respectively. The highest F*c* value appeared in the evening (19:20) in March, which was 0.2158 $μmol·m^{-2}·s^{-1}$. In April and May, it appeared at noon (13:35). They were 0.1148 μmol·m-

https://doi.org/10.5194/egusphere-2024-1226
Preprint. Discussion started: 1 July 2024

$^{2}\cdot s^{-1}$ and 0.1397 μmol·m^{-2}·s^{-1}, respectively.

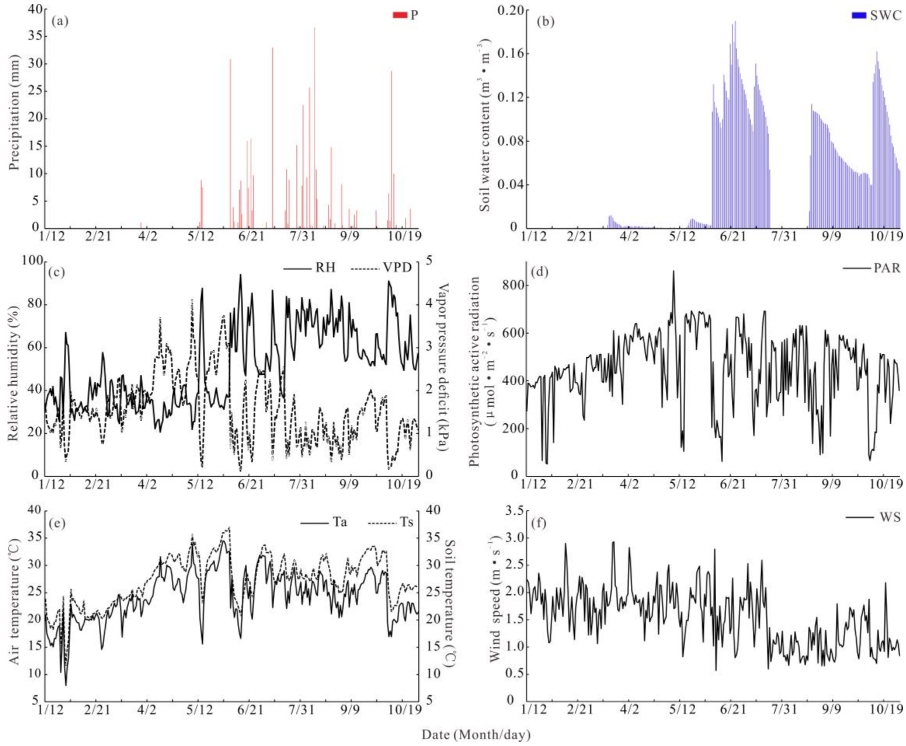

Figure 2 The variation characteristics of environmental factors in the study area.

The diurnal variation of the F*c* was characterized by a 'U'-shaped single-peak curve, which was stable at night and decreased first and then increased during the day (Fig. 3b), during the rainy season. At about 7:35 in the morning, with the increase of PAR intensity, the photosynthesis of the grassland ecosystem is continuously enhanced, and the F*c* begins to become negative. At this time, the grassland ecosystem changes from carbon emission at night to carbon absorption, forming the source of CO_2 absorption and reaching the maximum peak of carbon absorption at 10:00–14:00. Until about 17:20, the F*c* becomes positive again. The grassland ecosystem transitions into a state of carbon emission, releasing CO_2 into the atmosphere. The lowest F*c* values appeared in the morning (10:00–12:00) from the diurnal variation of flux in various months, which were –1.4286 μmol·m^{-2}·s^{-1}, –1.3834 μmol·m^{-2}·s^{-1}, and –1.0278 μmol·m^{-2}·s^{-1}, respectively. The highest F*c* values appeared in the evening (18:35–18:50), which were 0.7584 μmol·m^{-2}·s^{-1}, 0.4959 μmol·m^{-2}·s^{-1} and 0.5715 μmol·m^{-2}·s^{-1}, respectively.

3.3 Seasonal variation of CO_2 flux

From Fig.4, we can find that the seasonal variation of the F*c* in the grassland ecosystem was evident. In the dry season, the ecosystem experiences severe drought and water scarcity, leading to

https://doi.org/10.5194/egusphere-2024-1226
Preprint. Discussion started: 1 July 2024

poor growth of herbaceous plants, which is characterized by carbon emissions. The monthly cumulative CO_2 emission fluxes were 18.64 g·m^{-2}, 15.96 g·m^{-2}, and 20.64 g·m^{-2}, respectively, displaying an initial decline followed by a rise. The CO_2 emission flux was the highest in May. The ecosystem has abundant P in the rainy season, the SWC is high, the herbaceous plants are in the growing season, and the photosynthesis capacity is significant, so it is characterized by carbon sink function. The monthly cumulative CO_2 absorption fluxes were 6.42 g·m^{-2}, 24.41 g·m^{-2}, and 5.14 g·m^{-2}, respectively, displaying a rise initially followed by a decline, and the carbon absorption capacity in September was the most significant.

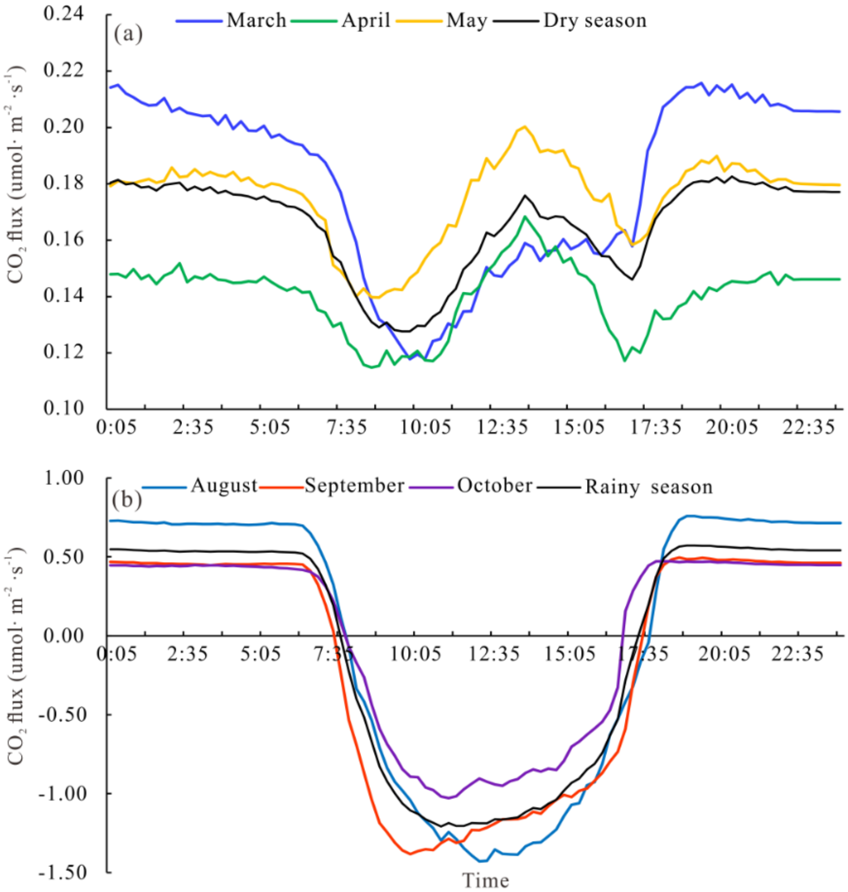

Figure 3 Diurnal variation characteristics of the F*c* (a–dry season; b–rainy season).

https://doi.org/10.5194/egusphere-2024-1226
Preprint. Discussion started: 1 July 2024

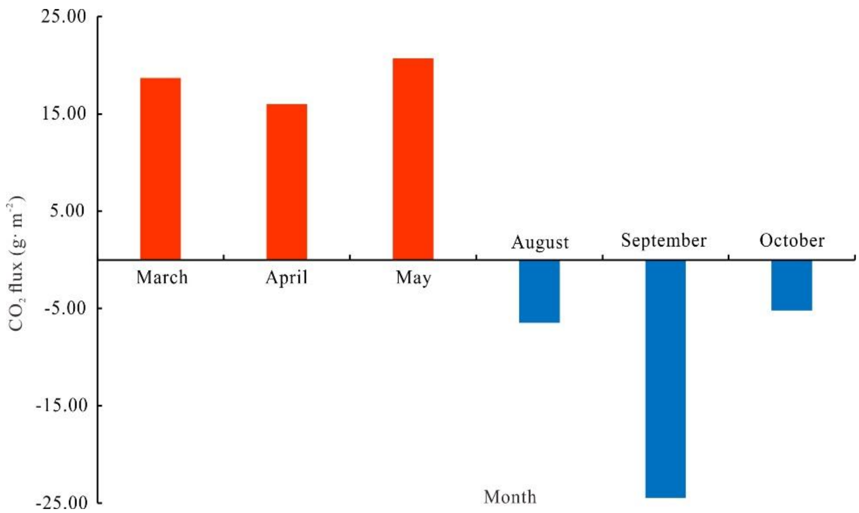

Figure 4 Monthly variation characteristics of the F*c*.

The existing observation data were averaged and calculated respectively in this study, and they were used as the daily mean F*c* of the two seasons in the whole year. According to the days of the dry season (213 days) and the rainy season (152 days) in the whole year, the dry season, rainy season, and annual F*c* of the grassland ecosystem were calculated. The findings indicated that the mean daily F*c* was 0.1632 $\mu mol \cdot m^{-2} \cdot s^{-1}$, and the cumulative CO_2 emission was 1.3215 $t \cdot ha^{-1}$ in the dry season. The daily average F*c* was –0.1062 $\mu mol \cdot m^{-2} \cdot s^{-1}$, and the cumulative CO_2 uptake was 0.6137 $t \cdot ha^{-1}$ in the rainy season. From the annual scale, the cumulative F*c* of the grassland ecosystem was 0.7078 $t \cdot ha^{-1} \cdot a^{-1}$ (0.1926 $t\ C \cdot ha^{-1} \cdot a^{-1}$), making it a weak carbon source.

3.4 The relationship between CO_2 flux and environmental factors

3.4.1 Response of CO_2 flux to PAR

This study selected carbon flux data and micrometeorological observation data corresponding to period and analyzed the mutual correlation between F*c* and environmental factors. The research area belongs to a typical semi-arid region, where vegetation growth and physiological processes are mainly regulated by temperature and moisture factors (Jiang et al., 2007; Fei et al., 2017a). Therefore, when analyzing the influencing factors of ecosystem CO_2 flux, we mainly selected environmental factors including P, SWC, Ts, Ta, RH, PAR, and VPD for pearson analysis. No significant correlation between PAR and F*c* during the dry season was indicated by the results of the pearson correlation analysis ($R = 0.180$, $P = 0.092$). Still, there was a strong negative correlation between PAR and F*c* during the rainy season ($R = -0.578$, $P < 0.01$), and this relationship was more obvious in Fig. 5a. As a key environmental factor driving plant photosynthesis, photosynthetically active radiation will directly affect the carbon absorption rate of grassland ecosystem and further affect the carbon budget pattern of ecosystem. In the rainy season, the F*c* of the grassland ecosystem decreased with the increase of PAR, and the carbon absorption capacity increased continuously, and the relationship between them could be expressed by formula (3). Secondly, when PAR was under 500 μmol·m^{-2}·s^{-1} (Fig. 5b), the NEE of the ecosystem decreases rapidly with increasing PAR. At the same time, the distribution of NEE with PAR was relatively concentrated. However, when PAR was above 500μmol·m^{-2}·s^{-1}, the magnitude of the decrease in NEE with increasing PAR gradually decreases, and the distribution of NEE with PAR was relatively scattered, indicating that the F*c* was also influenced by various other environmental factors present in the ecosystem when solar radiation is high. Once PAR reaches the light saturation point at 1523.64 μmol·m^{-2}·s^{-1}, the NEE of the ecosystem reached to its minimum, and the light response curve gradually begins to flatten. These research findings align with those of previous studies carried out in diverse grassland ecosystems (Zhao et al., 2007; Wang et al., 2015; Guo et al., 2022).

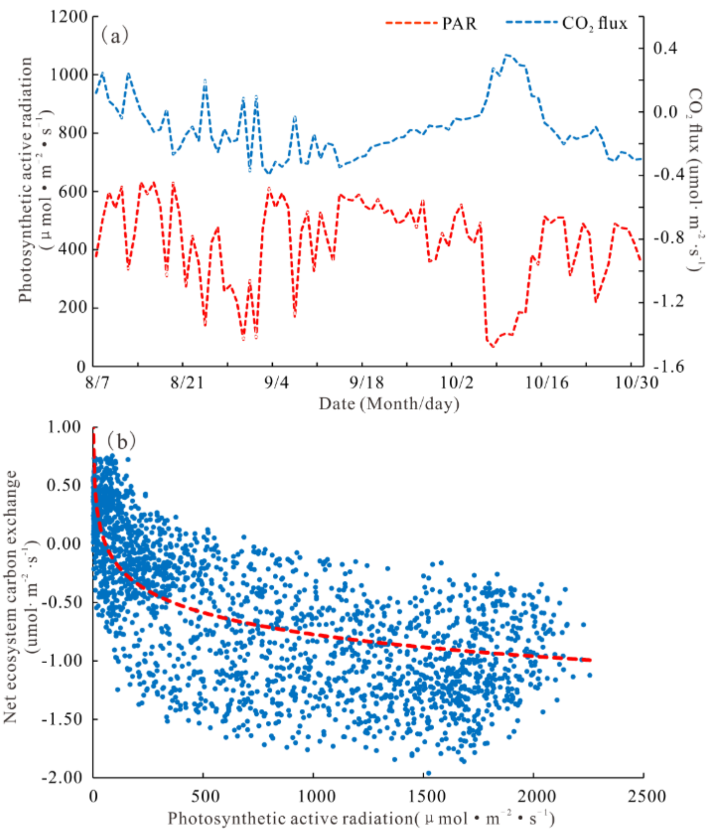

Figure 5 The correlation between PAR and F*c* (a–the relationship between PAR and F*c* in the rainy season; b–the response of F*c* to PAR during daytime in the rainy season).

https://doi.org/10.5194/egusphere-2024-1226
Preprint. Discussion started: 1 July 2024

3.4.2 Relationship with other environmental factors

With no significant correlation with SWC (Fig. 6a and 6b) shown by the daily scale F*c* of grassland ecosystems in the various seasons, there was a moderate negative correlation with Ta and Ts (*P*<0.01), a moderate positive correlation with P (*P*<0.01), and a strong positive correlation with RH (*P*<0.01). The daily scale F*c* in the dry season has a moderate negative correlation with VPD (*P*<0.01), while the F*c* in the rainy season shows a strong negative correlation with VPD (*P*<0.01). Throughout varying seasons, the F*c* increases with the increase of P and RH, as well as the decrease of Ta, Ts, and VPD. Due to the small variations in SWC within the two seasons (Fig. 2b), therefore, the impact of SWC on the diurnal fluctuation of the F*c* was not significant. In general, the diurnal variation of F*c* in the dry season is mainly affected by RH, while the rainy season is mainly affected by RH and VPD, and the influence of other environmental factors is generally weak.

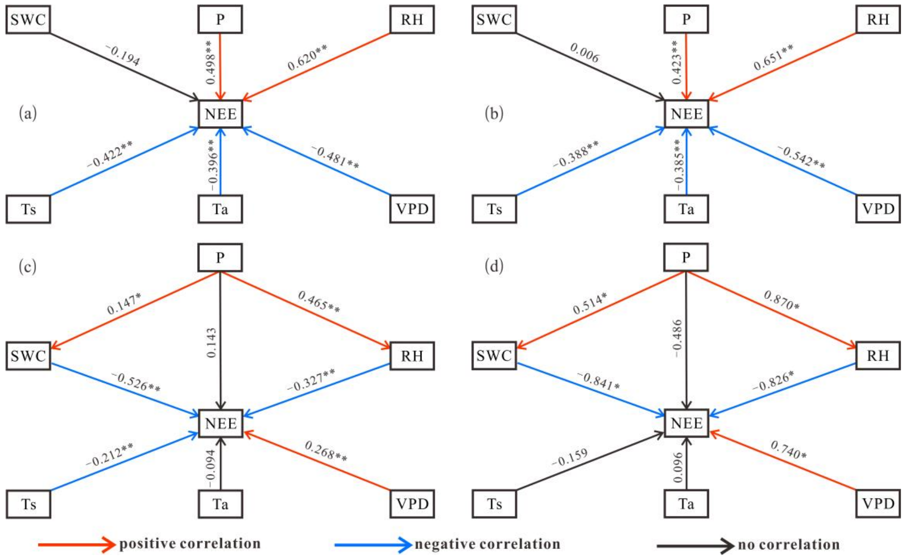

Figure 6 The pearson correlation between F*c* and environmental factors (a–daily scales of the dry season; b–daily scales of the rainy season; c–annual daily scales; d–monthly scales, the ** is *P*<0.01; the * is *P*<0.05).

Throughout the year on a daily scale (Fig. 6c), the F*c* showed no significant correlation with Ta and P, a weak positive correlation with VPD (*P*<0.01), a weak negative correlation with Ts (*P*<0.01), a moderate negative correlation with RH (*P*<0.01), and a strong negative correlation with SWC (*P*<0.01). It is evident that as the time series extends, the physiological responses of photosynthesis and respiration processes in the grassland ecosystem to specific environmental factors have undergone changes. As the VPD decreases, and RH, SWC, and Ts increase, and the F*c* of ecosystem decreased gradually. Particularly, the impact of SWC was most significant, closely related to the distinct climatic characteristics of wet and dry seasons in the study area. Under such

https://doi.org/10.5194/egusphere-2024-1226
Preprint. Discussion started: 1 July 2024

climatic conditions, the variation in SWC throughout the year becomes the dominant factor restricting regional vegetation growth and recovery (Jiang et al., 2007), significantly influencing the intra-annual variation of the F*c*.

The study also found that at the monthly scale, the F*c* showed no significant correlation with Ta, Ts, and P (Fig. 6d), but exhibits a strong negative correlation with SWC and RH (P<0.05), and a strong positive correlation with VPD (P<0.05). As the temporal scale increases, the environmental driving factors influencing the variation in F*c* decrease, but the correlation significantly increases. This may be attributed to the short monthly time series of the observational data. In general, at the monthly scale, SWC, RH, and VPD emerge as the predominant factors influencing the variation in F*c* within the ecosystem. Furthermore, the change in time scale will also affect the correlation between F*c* and driving factors, aligning with the findings in Heihe River Basin (Bai et al., 2022).

4 Discussion

4.1 Carbon flux of grassland ecosystem

The herbs in the study area are mainly C_4 plants (Grace et al., 1995), which are called high-efficiency photosynthetic plants, and the C_4 plants exhibit higher efficiency in photosynthesis and resource utilization when compared to C_3 plants (Cui et al., 2021; Arslan et al., 2023; Xu et al., 2023). However, similar to other savanna ecosystems, the study area has been in a dry, high-temperature, and low-rainy climate for a long time. This extreme climatic condition makes the productivity of C_4 herbaceous plants only maintain at a medium level (Grace et al., 1995), therefore, the carbon sink capacity is relatively weak. The data analysis revealed that within the grassland ecosystem situated in the study area, the daily maximum CO_2 uptake rate was recorded at only 1.4286 $\mu mol \cdot m^{-2} \cdot s^{-1}$, which stands notably lower in comparison to other grasslands found in arid and semi-arid regions (Fig. 7) (Li et al., 2005; Kato et al., 2006; Du et al., 2012; Hu et al., 2018; Niu et al., 2018; Zhang et al., 2020; Guo et al., 2022).

Through comparative analysis, it can be observed that various grasslands in arid/semi-arid regions primarily function as carbon sinks, but some grasslands also show the characteristics of carbon emissions (Table 2). Simultaneously, most savanna ecosystems globally demonstrate carbon sequestration features (Table 2), with only a few exhibiting characteristics of carbon emissions, with the NEE varying from around 1.28 to –3.87 t C$\cdot ha^{-1} \cdot a^{-1}$. Consistent with findings from other savanna ecosystems (Grace et al., 1995; Miranda et al., 1997; Fei et al., 2017a), the special hydrothermal conditions make the vegetation growth of the grassland in the study area exhibiting pronounced seasonal characteristics and affect the change of carbon flux. In the season of drought and water

https://doi.org/10.5194/egusphere-2024-1226
Preprint. Discussion started: 1 July 2024

shortage, the herbs growth is poor, and the ecosystem mainly emits carbon, showing a carbon source characteristic. During the rainy season, the vegetation enters the peak period of growth, with strong carbon fixation ability, and the ecosystem mainly absorbs carbon, showing a carbon sink function. Overall, the grassland ecosystems in the study area predominantly exhibit carbon emissions, albeit at relatively low levels, demonstrating a carbon-neutral attribute. The carbon flux characteristics are the same as those of Sumbrugu Aguusi savanna grassland in Sudan (Quansah et al., 2015), Kruger Park semi-arid savanna in South Africa (Archibald et al., 2009) and Virginia Park semi-arid savanna in Australia (Hutley et al., 2005).

Through comparative analysis, we found that most of the grasslands in the savanna ecosystem and arid and semi-arid areas are dominated by carbon sinks. The reason for the carbon emission status of grassland in this study may be related to the continuous reduction of rainfall in the study area in recent years (Fig. 8). Under this extremely dry and rainless climate condition, the carbon sequestration capacity of herbaceous plants with low vegetation productivity is significantly reduced. In the case of continuous reduction of rainfall in the future, the carbon emissions of grassland ecosystems in the study area may continue to increase. At the same time, the study area as a special heat island habitat in the global temperate zone. Under the climate scenario of continuous warming and decreasing precipitation in the future, the vegetation community structure in some temperate regions will succession to the savanna vegetation community. With the extension of drought and high temperature, grassland ecosystems in these areas may change from carbon sinks to carbon sources, which is extremely important for the carbon balance of global terrestrial ecosystems.

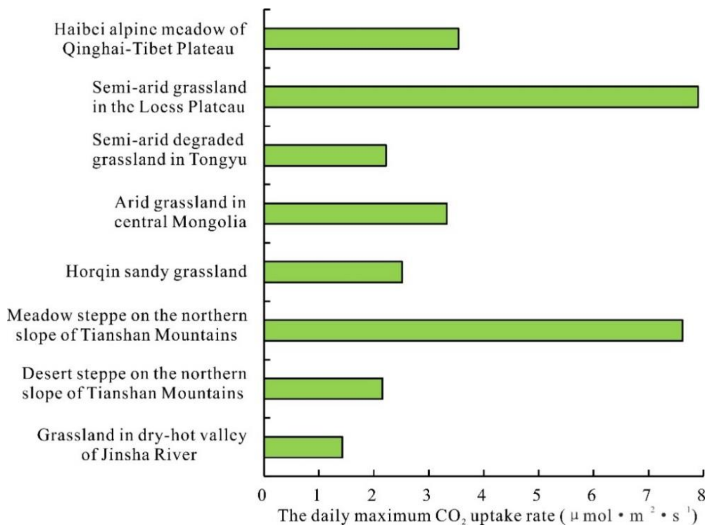

Figure 7 The daily maximum CO_2 uptake rate of different grassland ecosystems.

https://doi.org/10.5194/egusphere-2024-1226
Preprint. Discussion started: 1 July 2024

Table 2 Comparison of NEE in grassland ecosystems and savanna ecosystems.

Country	Location	Latitude &longitude	Vegetation	NEE $(t\ C \cdot ha^{-1} \cdot a^{-1})$	References
China	Meitang	26°4'6.24" N, 107°28'12" E	subtropical grassland	–1.16	Sun et al., 2020
	Heihe Dashalong Observation Station	38°50'23.64" N, 98°56'16" E	marsh alpine meadow	–3.08	Bai et al., 2022
	Heihe Arou Observation Station	38°2'50.28" N, 100°27'51.48" E	alpine meadow	–2.28	
	Xilin River Basin	43°33'N, 116°40'E	semi-arid grassland	–0.61	Du et al., 2012
	Semi-arid Climate and Environment Observatory	35°57'N, 104°08'E	semi-arid grassland	–0.99	
	Tongyu Degraded Grassland Observatory	44°25'N, 122°52'E	semi-arid grassland	–0.37	
	Yunwu Mountain National Nature Reserve	36°19'N, 106°28'E	semi-arid grassland	–0.02	Zhang et al., 2020
	Naiman Desertification Research Station	42°55'N, 120°42'E	sandy grassland	0.91	Niu et al., 2018
	Naiman Desertification Research Station	42°55'N, 120°42'E	enclosure of sandy grassland	0.96	Chen et al., 2019
	Qinghai Lake	36°42'N, 100°46'E	*Kobresia tibetica* wet meadow	0.55	Wu et al., 2018
	Jinsha River Field Observation Station	26°4'6.24" N, 101°49'41.68" E	grassland savanna	0.19	This study
	Yuanjiang	23°28'26"N, 102°10'39"E	semi-arid savanna	–1.30	Fei et al., 2017b
	Yanchi Research Station	37°42.51'N, 107°13.62'E	semi-arid shrub	–0.77	Law et al., 2002
Sudan	Northwestern Benin	09°44'24"N, 01°36'00"E	cultivated savanna	–2.32	Ago et al., 2014
	Bontioli	10°51'56"N, 03°4'22"W	trees and shrub savanna	–3.04	Brümmer et al., 2008
	Kayoro Dakorenia	10°55'4.8"N, 01°19'15.6"W	fallow and cropland	1.08	Quansah et al., 2015
	Nazinga Park	11°09'7.20"N, 1°35'9.6"W	nature reserve savanna	–3.87	
	Sumbrugu Aguusi	10°50'45.6"N, 0°55'1.2"W	grassland savanna	1.28	
South Africa	Kruger Park	/	semi-arid savanna	0.25	Archibald et al., 2009
	Ca. 20 km east of Maun, Botswana	19°54'S, 23°33'E	woodland savanna	–0.12	Veenendaal et al., 2004
West Africa	Dahra field site	15°24'00"N, 15°24'48"W	shrub and tree savanna	–2.71	Tagesson et al., 2015
Brazil	Reserva Ecológica do IBGE	15°56'S, 47°51'W	trees and shrubs	–2.88	Santos et al., 2003
Spain	El Llano de los Juanes	36°55'41.7"N, 02°45'1.7"W	mediterranean shrubland	–0.02	Serrano-Ortiz et al., 2009
United States	Tonzi Ranch, California	38°25'48"N, 120°57'00"W	oak and grass savanna	–0.98	Ma et al., 2003
Australia	Virginia Park	19°53'00"S, 146°33'14"E	semi-arid savanna	0.21	Hutley et al., 2005
	Howard Springs	12°30'24"S, 131°5'24"E	mesic savanna	–1.55	
	Pine Hill cattle station	22°16'48"S, 133°15'00"E	woodland savanna	–1.25	Cleverly et al., 2013
	Central Australia	22°18'00"S, 133°12'00"E	acacia savanna	–2.58	Eamus et al., 2013
	Howard Springs	12°29.71'S, 131°09.03'E	open-forest savanna	–3.60	Beringer et al., 2007

https://doi.org/10.5194/egusphere-2024-1226
Preprint. Discussion started: 1 July 2024

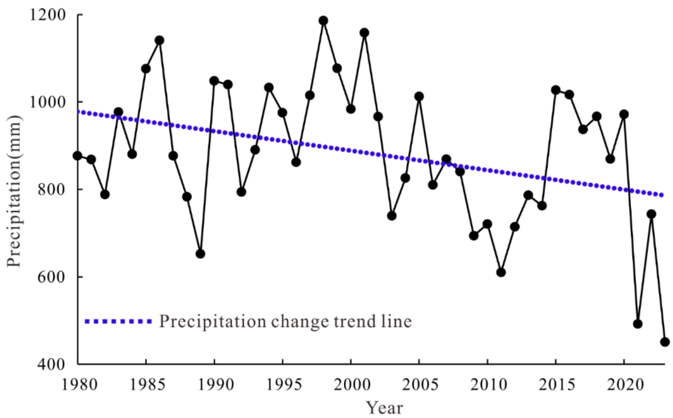

Figure 8 The precipitation changes in the study area from 1980 to 2023 (The precipitation data from 1980 to 2022 are collected from Yunnan Statistical Yearbook, and the precipitation data in 2023 were the measured data of Jinsha River Field Observation Station.).

4.2 Effects of environmental factors on CO_2 flux

4.2.1 Temperature factor

As a crucial environmental factor influencing the F*c* of ecosystems, temperature mainly affects the F*c* of terrestrial ecosystems by regulating biological activities such as photosynthesis and respiration (Woodwell et al., 1983; Pan et al., 2020; Johnston et al., 2021; Chen et al., 2023), especially for grassland ecosystems, several prior studies have validated that temperature serves as the primary driving force controlling the variation in F*c*. Nevertheless, owing to variations in climate and environmental conditions, the regulatory impact of temperature fluctuations on the F*c* differs significantly across various types of grassland ecosystems. Compared with temperate grassland and semi-arid grassland, the warming effect has the most significant impact on the carbon flux of frigid grasslands worldwide. However, in semi-arid grassland ecosystems, the effect of warming is not significant (Wang et al., 2019). The rise in temperature (both annual average temperature and annual average soil temperature) reduced the carbon flux of temperate grasslands in China, while the effect on alpine grasslands was opposite (Liu et al., 2024). In the Inner Mongolia Plateau, with the increase of temperature, the NEE of the grassland ecosystem will increase (Liu et al., 2018), while the change of Qinghai–Tibet Plateau, compared with it, is very small, and there is no correlation between F*c* and temperature change in the Inner Mongolia grassland during the drought period (Hao et al., 2006). Ta and Ts exhibit a negative correlation with the F*c* at different seasonal daily scales in the grassland ecosystem in dry-hot valley of JS, similar to the control mechanisms seen in other arid and semi-arid grasslands (Li et al., 2015; Niu et al., 2018; Chen et al., 2019). As the time series extends and the temporal scale increases, the impact of Ta and Ts on the fluctuations in the F*c* in the grassland

https://doi.org/10.5194/egusphere-2024-1226
Preprint. Discussion started: 1 July 2024

of study region continues to weaken, which is related to the small differences in Ta and Ts within different time scales in the study area. That is, the small temperature difference leads to the distribution change of the F*c* in time is not sensitive to temperature fluctuation, which is the same as the characteristics of the savanna ecosystem in YJ (Fei et al., 2017a). This phenomenon is also common in other arid regions (Wang et al., 2021).

4.2.2 Water factor

Previous studies have pointed out that a potential limiting factor affecting carbon uptake in terrestrial ecosystems is soil moisture, which can diminish NPP through water stress in ecosystems, leading to vegetation death (Green et al., 2019). Simultaneously, soil moisture may exacerbate extreme climatic conditions through the intricate interaction between the land and the atmosphere. Particularly in arid regions characterized by scarce water resources, there exists a significant interaction between soil moisture and vegetation. Hence, in terms of carbon and water fluxes affecting dryland ecosystems, SWC is a more important ecosystem control factor than Ta (Zhang et al., 2012; Zou et al., 2016; Fei et al., 2017a; Tarin et al., 2020; Kannenberg et al., 2024). For instance, in the herbs growth season of the Qinghai–Tibet Plateau, regions with plentiful precipitation in the east and southeast primarily regulate carbon absorption capacity through temperature. Conversely, SWC emerges as the principal determinant of carbon sequestration capability in the arid and water shortage western region (Wang et al., 2021). Simultaneously, the SWC emerges also as the predominant factor influencing the daily fluctuations of NEE in grassland ecosystems in the semi-arid regions of northern China (Zhao et al., 2020). In the sandy grasslands of Horqin, the NEE during the plant growth season increases with the rise in SWC, while it decreases during the non-growth season (Chen et al., 2019). The research area is a classic dryland ecosystem characterized by scarce and concentrated precipitation. The driving effect of water on the ecosystem is obvious. Plant physiology is greatly affected by water stress. Higher SWC is conducive to promoting the recovery and growth of herbs (Jiang et al., 2017), and this enhancement in vegetation growth contributes significantly to augmenting the carbon sink capacity. Therefore, it can be observed that in the season with more rainfall, the study area has a carbon sink function due to higher SWC (Figure 2b), whereas in the dry season, it exhibits characteristics of carbon emissions.

In arid ecosystem, alterations in the P significantly affect plants and soil, especially the grassland ecosystem has the greatest response to the change of the P. The effectiveness of water dictates plants growth and the release and absorption of CO_2. Therefore, prior researches have indicated that the F*c* of grasslands in arid regions exhibits greater sensitivity to variations in the P (Knapp et al., 2002; Niu et al., 2007; Weltzin et al., 2003; Zhang et al., 2020). An increase in the P

https://doi.org/10.5194/egusphere-2024-1226
Preprint. Discussion started: 1 July 2024

led to a delay in the peak of gross primary productivity in vegetation growth stage of the Inner Mongolia desert steppe, enhancing the ecosystem's carbon flux (Li et al., 2017; Zhang et al., 2019). The decrease of the P significantly reduced the soil respiration in the early and middle vegetation growth season of Horqin sandy grassland (Wang et al., 2023). The P of Xilinhot grassland changed the F*c* in the vegetation growth season mainly by affecting SWC (Wang et al., 2015). High water levels (annual average precipitation and soil moisture) have continuously increased the carbon flux of temperate grasslands and alpine grasslands in the Mongolian Plateau, Loess Plateau, and Qinghai–Tibet Plateau (Liu et al., 2024).

Changes in hydrological conditions such as the P and SWC can significantly affect the water balance characteristics and water redistribution of the savanna ecosystems due to the arid and hot climate environment characteristics, thereby altering the ecological system structure and vegetation community composition of woody and herbaceous plants coexisting (Yu et al., 2015; Lee et al., 2018; Jin et al., 2019; Zhang et al., 2019; Hoffmann, 2023; Mattos et al., 2023), thereby affecting vegetation productivity (Jin et al., 2018), ecological water use efficiency (Yu et al., 2015; Lee et al., 2018; Mattos et al., 2023), plant diversity (He, et al., 2024), and carbon flux (Fei et al., 2017a). Changes in hydrothermal conditions have formed the distinct vertical zonation structure of vegetation communities in the savanna of the JS (He, et al., 2024). The continuous decrease in the P led to a marked reduction in both the average height and coverage of the herbaceous community in the YJ. However, it significantly increased the species richness and evenness index of the herbaceous community (Jin et al., 2019). Observations of the F*c* showed that the P determined the carbon sink change of the savanna ecosystem in the YJ (Fei et al., 2017a). As for the study area, the P shows a positive correlation with the F*c* at different seasonal daily scales, with no significant relationship observed with the F*c* variation on the daily and monthly scales throughout the year. However, the variation in P significantly affects the regional SWC and RH (Fig. 6c and 6d). Therefore, we suggests that the impact mechanism of the P on the F*c* in the JS dry-hot valley grassland ecosystem may be similar to that of the Xilinhot grassland ecosystem, where the P mainly controls vegetation growth by affecting SWC and RH, thereby indirectly influencing the F*c* in the grassland ecosystem.

4.2.3 Relative humidity and vapor pressure deficit factor

The arid/semi-arid grassland ecosystem is short of water resources, the soil nutrients are relatively poor, and the ecosystem is fragile and sensitive. Especially with the change in global climate, RH has become a key limiting factor restricting its sustainable development (Wang et al., 2023). As an important measure of atmospheric dryness, the fluctuation of VPD is controlled by RH

https://doi.org/10.5194/egusphere-2024-1226
Preprint. Discussion started: 1 July 2024

and has a high correlation with other important driving factors of ecosystem productivity, such as Ta and SWC, which is a key climate regulation factor affecting ecosystem photosynthesis and transpiration. Multiple studies have shown that when RH decreases, vegetation stomata will be closed due to an increase in VPD, thereby preventing excessive water loss (Williams et al., 2013; Novick et al., 2016; Sulman et al., 2016; Hsu et al., 2021), leading to a decrease in the photosynthetic rate of leaves and canopies，thereby inhibiting photosynthesis (McDowell et al., 2015; Sulman et al., 2016; Yuan et al., 2019), reducing vegetation productivity and hindering vegetation growth. Therefore, there is a mainly negative correlation between the intensity of plant photosynthesis and VPD. Zhong et al. (2023) discovered that excluding the influences of Ta and soil moisture on vegetation productivity, VPD negatively impacts vegetation productivity in the majority of Northern Hemisphere regions. Globally, studies have also shown that increased VPD reduces global vegetation growth and offsets the beneficial impacts of CO_2 fertilization (Yuan et al., 2019). Simultaneously, the interannual variation of VPD shows a significant negative correlation with net ecosystem productivity and affects the interannual variation of atmospheric CO_2 growth rate (He et al., 2022). Because of variations in climatic conditions and the synergistic effects of multiple environmental factors, the response mechanisms of the F*c* in different grassland ecosystems to changes in VPD and RH are also varied. For instance, in the savanna ecosystem of YJ, the F*c* shows a negative correlation with VPD (Fei et al., 2017a). Wang et al. (2021) found through a study on the spatial variation of carbon flux of 10 distinct grassland types that a positive correlation exists between VPD and NEE in the Qinghai–Tibet Plateau. In the arid grasslands of Heihe River Basin (Bai et al., 2022), the F*c* is positively correlated with VPD and RH. The F*c* at the daily scale exhibit a positive correlation with RH and a negative correlation with VPD during different seasons in the study area. Taking into account the seasonal changes in different environmental factors (Fig. 2c), during the dry season, the RH is low, VPD is high. The ecosystem exhibits a carbon emission state, while the opposite is observed during the rainy season. Generally, the reduction in RH and the increase in VPD will inhibit the ecosystem’s carbon absorption capacity.

5 Conclusions

This study quantitatively analyzed the F*c* variations and their relationships with environmental factors in the grassland ecosystem of the dry-hot valley of JS, enriching the theoretical understanding of key carbon cycling processes in the savanna ecosystem in China. Nonetheless, the absence of long-term observational data on the F*c* in our study precludes a more thorough examination of the inter-annual variation characteristics of the F*c*. Secondly, the study did not

https://doi.org/10.5194/egusphere-2024-1226
Preprint. Discussion started: 1 July 2024

effectively observe the dynamic characteristics of soil respiration, making it impossible to accurately calculate the GPP of the ecosystem. Furthermore, we only observed and studied the changes in F*c* of the grassland ecosystem, while the savanna ecosystem has a vegetation community structure with two levels of shrub and grass. Therefore, forthcoming our research will emphasize the extended observation of the F*c* changes in the savanna ecosystem with a complete vegetation community structure, especially the use of eddy correlation methods to expand the scope of ecosystem observation and reduce the uncertainty of measurement samples, so as to better clarify the carbon budget pattern of the ecosystem. Through this research, we have arrived at the following findings:

(1) The diurnal variation of F*c* showed a ‘W’ shaped bimodal curve during the dry season. The maximum daily CO_2 emission rate reached 0.2158 $\mu mol \cdot m^{-2} \cdot s^{-1}$ in March, with the highest cumulative CO_2 emission of 20.64 $g \cdot m^{-2}$ observed in May. During the rainy season, the diurnal variation of F*c* in the ecosystem showed a ‘U’ shaped unimodal curve. The maximum daily CO_2 absorption rate reached 1.4286 $\mu mol \cdot m^{-2} \cdot s^{-1}$ in August, with the highest cumulative CO_2 absorption of 24.41 $g \cdot m^{-2}$ observed in September.

(2) In the rainy season existed a notable correlation between PAR and F*c*. Especially during the daytime, the relationship between F*c* and PAR followed a rectangular hyperbolic model. When PAR reached the light saturation point, the photosynthetic rate of the ecosystem would peak, and the light response curve would gradually level off. Additionally, when PAR was high, the F*c* of the ecosystem was also impacted by other driving factors.

(3) The diurnal variation of F*c* in the dry season is mainly affected by RH, while the rainy season is mainly affected by RH and VPD. Small temperature differences result in a relatively weak overall impact of Ta and Ts on the F*c* of the ecosystem. P mainly indirectly controls the vegetation growth and the F*c* by influencing SWC and RH. Overall, SWC, RH, and VPD were the main environmental factors influencing the F*c*. As SWC and RH rise while VPD declines, the ecosystem’s carbon absorption capacity experiences a notable enhancement.

(4) Affected by environmental factors, the F*c* of the grassland ecosystem exhibited significant seasonal characteristics. During the dry season, the ecosystem showed carbon emissions, with a cumulative CO_2 emission of 1.3215 $t \cdot ha^{-1}$. During the rainy season, the ecosystem showed carbon absorption, with a cumulative CO_2 absorption of 0.6137 $t \cdot ha^{-1}$. Throughout the year, the ecosystem was a weak carbon source. In the case of continuous reduction of P in the future, the carbon emissions of the ecosystem may continue to increase.

Data availability

https://doi.org/10.5194/egusphere-2024-1226
Preprint. Discussion started: 1 July 2024

The CO_2 flux data and environmental data used to support the findings of this study were available from the corresponding author upon request. The administrative boundary data (DOI:10.12078/2023010101; DOI:10.12078/2023010103) and river data (DOI:10.12078/2018060101) were downloaded from the RESDC from the Chinese Academy of Sciences (https://www.resdc.cn/Default.aspx).

Author contributions

All authors were involved in the preparation and design of the manuscript. Chaolei Yang wrote the manuscript, and all authors provided feedback and suggestions for revision. Yufeng Tian and Jingqi Cui processed and analyzed the research data. Zong Wei, Yong Huang, and Aihua Jiang are mainly responsible for the daily maintenance and data collection of monitoring instruments. All the authors have read and passed the final manuscript.

Competing interests

The authors has declared that no conflict of interest.

Financial support

This study received funding from the China Geological Survey (grant nos. DD20220888) and the National Natural Science Foundation of China (grant nos. U2102209).

References

Archibald, S.A., Kirton, A., van der Merwe, M.R., Scholes, R.J., Williams, C.A., Hanan, N.: Drivers of inter-annual variability in net ecosystem exchange in a semi-arid savanna ecosystem, South Africa, Biogeosci, 6, 251–266, 2009.

Ago, E.E., Agbossou, E.K., Galle, S., Cohard, J.M., Heinesch, B., Aubinet, M.: Long term observations of carbon dioxide exchange over cultivated savanna under a Sudanian climate in Benin (West Africa), Agric. For. Meteorol, 197, 13–25, https://doi.org/10.1016/j.agrformet.2014.06.005, 2014.

Arslan, A.M., Wang, X., Liu, B.Y., Xu, Y.N., Li, L., Gong, X.Y.: Photosynthetic resource-use efficiency trade-offs triggered by vapour pressure deficit and nitrogen supply in a C_4 species, Plant Physiol. Biochem, 197, 107666, https://doi.org/10.1016/j.plaphy.2023.107666, 2023.

Bousquet, P., Ciais, P., Miller, J.B., Dlugokencky, E.J., Hauglustaine, D.A., Prigent, C., White, J.: Contribution of anthropogenic and natural sources to atmospheric methane variability, Nature, 443, 439–443, https://doi.org/10.1038/nature05132, 2006.

Beringer, J., Hutley, L.B., Tapper, N.J., Cernusak, L.A.: Savanna fires and their impact on net ecosystem productivity in North Australia, Global Change Biol, 13, 990–1004, https://doi.org/10.1111/j.1365-2486.2007.01334.x, 2007.

Brümmer, C., Falk, U., Papen, H., Szarzynski, J., Wassmann, R., Brüggemann, N.: Diurnal, seasonal, and interannual variation in carbon dioxide and energy exchange in shrub savanna in Burkina Faso (West Africa), J. Geophys. Res.: Biogeosci, 113, https://doi.org/Artn

https://doi.org/10.5194/egusphere-2024-1226
Preprint. Discussion started: 1 July 2024

G0203010.1029/2007jg000583, 2008.
Bai, Y.F., Cotrufo, M.F.: Grassland soil carbon sequestration: current understanding, challenges, and solutions, Science, 377, 603–608, https://doi.org/10.1126/science.abo2380, 2022.
Bai, X.J., Wang, X.F., Liu, X.H., Zhou, X.Q.: Dynamics and driving factors of carbon fluxes in wetland，cropland and grassland ecosystems in Heihe river basin, Remote Sens, Technol. Appl, 37, 94−107, https://doi.org/10.11873/j.issn.1004-0323.2022.1.0094, 2022.
Bai, X.Y., Zhang, S.R., Li, C.J., Xiong, L., Song, F.J., Du, C.C., Li, M.H., Luo, Q., Xue, Y.Y., Wang, S.J.: A carbon-neutrality-capacity index for evaluating carbon sink contributions, Environ. Sci. Ecotechnol., 15, 100237, https://doi.org/10.1016/j.ese.2023.100237, 2023.
Bureau of Statistics of Yunnan Province. Yunnan Statistical Yearbook; China Statistics Press: Beijing, China, 2023.
Campbell, G.S., Norman, J.M.: An introduction to environmental biophysics, Springer Sci, Business Media, 2012.
Cleverly, J. Boulain, N., Villalobos-Vega, R., Grant, N., Faux, R., Wood, C., Cook, P.G., Yu, Q., Leigh, A., Eamus, D.: Dynamics of component carbon fluxes in a semi-arid Acacia woodland, central Australia, J. Geophys. Res.: Biogeosci, 118, 1168–1185, https://doi.org/10.1002/jgrg.20101, 2013.
Chen, Y.P., Niu, Y.Y., Li, W., Li, Y.Q., Gong, X.W., Wang, X.Y.: Characteristics of carbon flux in sandy grassland ecosystem under natural restoration in Horqin sandy land, Plateau Meteorol, 38, 650–659, https://doi.org/10.7522/.issn.1000-0534.2018.00133, 2019.
Cui, H.C.: Challenges and approaches to crop improvement through C_3-to-C_4 engineering, Front. Plant Sci, 12, 715391, https://doi.org/10.3389/fpls.2021.715391, 2012.
Chen, W.N., Wang, S., Wang, J.S., Xia, J.Y., Luo, Y.Q., Yu, G.R., Niu, S.L.: Evidence for widespread thermal optimality of ecosystem respiration, Nat. Ecol. Evol, 7, 1379–1387, https://doi.org/10.1038/s41559-023-02121-w, 2023.
Du, Q., Liu, H.Z., Feng, J.W., Wang, L., Huang, J.P., Zhang, W., Bernhofer, C.: Carbon dioxide exchange processes over the grassland ecosystems in semiarid areas of China, Sci. China, Ser. D Earth Sci, 42, 711–722, https://doi.org/10.1007/s11430-011-4283-1, 2012.
Dobson, A., Hopcraft, G., Mduma, S., Ogutu, J.O., Fryxell, J., Anderson, M., Archibald, S., Lehmann, C., Poole, J., Caro, T., Mulder, M.B., Holt, R.D., Berger, J., Rubenstein, D.I., Kahumbu, P., Chidumayo, E.N., Milner-Gulland, E.J., Schluter, D., Otto, S., Balmford, A., Wilcove, D., Pimm, S., Veldman, J.W., Olff, H., Noss, R., Holdo, R., Beale, C., Hempson, G., Kiwango, Y., Lindenmayer, D., Bond, W., Ritchie M., Sinclair, A.R.E.: Savannas are vital but overlooked carbon sinks, Science, 375, 392, https://doi.org/10.1126/science.abn4482, 2022.
Deng, Y.: The boundary definition and studyon the land use/cover change and landscape pattern of the dry-hot valley in Hengduan Mountains, Yunnan University, https://doi.org/10.27456/d.cnki.gyndu.2022.000408, 2022.
Eamus, D., Hutley, L.B., O'Grady, A.P.: Daily and seasonal patterns of carbon and water fluxes above a north Australian savanna, Tree Physiol, 21, 977–988, 2001.
Fang, J.Y., Guo, Z.D., Piao, S.L., Chen, A.P.: Terrestrial vegetation carbon sinks in China, 1981–2000. Sci. China Ser. D: Earth Sci, 50, 1341–1350, https://doi.org/10.1007/s11430-007-0049-1, 2007.
Fei, X.H., Song, Q.H., Zhang, Y.P., Liu, Y.T., Sha, L.Q., Yu, G.R., Zhang, L.M., Duan, C.Q., Deng, Y., Wu, C.S., Lu, Z.Y., Luo, K., Chen, A.G., Xu, K., Liu, W.W., Huang, H., Jin, Y.Q., Zhou,

R.W., Li, J., Lin, Y.X., Zhou, L.G., Fu, Y., Bai, X.L., Tang, X.H., Gao, J.B., Zhou, W.J., Grace, J.: Carbon exchanges and their responses to temperature and precipitation in forest ecosystems in Yunnan, Southwest China, Sci. Total Environ, 616–617, 824–840, https://doi.org/10.1016/j.scitotenv.2017.10.239, 2017a.

Fei, X.H., Jin, Y.Q., Zhang, Y.P., Sha, L.Q., Liu, Y.T., Song, Q.H., Zhou, W.J., Liang, N.S., Yu, G.R., Zhang, L.M., Zhou, R.W., Li, J., Zhang, S.B., Li, P.G.: Eddy covariance and biometric measurements show that a savanna ecosystem in Southwest China is a carbon sink, Sci Rep, 7, 41025, https://doi.org/10.1038/srep41025, 2017b.

Grace, J., Lloyd, J., McIntyre, J., Miranda, A.C., Meir, P., Miranda, H., Moncrieff, J.M., Massheder, J., Wright, I.R., Gash, J.: Fluxes of carbon dioxide and water vapour over an undisturbed tropical forest in south-west Amazonia, Global Change Biol, 1, 1–12, https://doi.org/10.1111/j.1365-2486.1995.tb00001.x, 1995.

Grace, J., José, J. S., Meir, P., Miranda, H. S., Montes, R.A.: Productivity and carbon fluxes of tropical savannas, J. Biogeogr, 33, 387–400, https://doi.org/10.1111/j.1365-2699.2005.01448.x., 2006.

Green, J. K., Seneviratne, S. I., Berg, A. M., Findell, K. L., Hagemann, S., Lawrence, D. M., Gentine, P.: Large influence of soil moisture on long-term terrestrial carbon uptake, Nature, 565, 476–479, https://doi:10.1038/s41586-018-0848-x, 2019.

Guo, W.Z., Jing, C.Q., Deng, X.J., Chen, C., Zhao, W.K., Hou, Z.X., Wang, G.X.: Variations in carbon flux and factors influencing it on the northern slopes of the Tianshan Mountains, Acta Prataculturae Sin, 31, 1−12. https://doi.org/10.11686/cyxb2021137, 2022.

He, Y.B., Lu, P.Z., Zhu, T.: Causes for the formation of dry-hot valleys in Hengduan Mountain-Yunnan plateau, Resour. Sci, 22, 69–72, https://www.resci.cn/CN/Y2000/V22/I5/69, 2000.

Houghton, R.A.: Counting terrestrial sources and sinks of carbon, Clim. Change, 48, 525–534, https://doi.org/10.1023/A:1005658316062, 2001.

Hutley, L.B., Leuning, R., Beringer, J., Cleugh, H.A.: The utility of the eddy covariance techniques as a tool in carbon accounting: tropical savanna as a case study, Aust. J. Bot, 53, 663–675, https://doi.org/10.1071/Bt04147, 2005.

Hao, Y.B., Wang, Y.F., Sun, X.M., Huang, X.Z., Cui, X.Y., Niu, H.S., Zhang, Y.H., Yu, G.R.: Seasonal variation in carbon exchange and its ecological analysis over Leymus chinensis steppe in Inner Mongolia, Sci. China, Ser. D Earth Sci, 49, 186–195, https://doi.org/10.1007/s11430-006-8186-5, 2006.

Hu, Y., Zhu, X.P., Jia, H.T., Han, D.L., Hu, B.A., Li, D.P.: Effects of fencing on ecosystem crabon exchange at meadow steppe in the northern slop oh the Tianshan Mountains, Chinese J. Plant Eco, 42, 372–381, https://doi.org/10.17521/cjpe.2016.0049, 2018.

Hsu, P.K., Takahashi, Y., Merilo, E., Costa, A., Zhang, L., Kernig, K., Lee, K.H., Schroeder, J.I.: Raf-like kinases and receptor-like (pseudo)kinase GHR1 are required for stomatal vapor pressure difference response, PNAS, 118, e2107280118, https://doi.org/10.1073/pnas.21072801, 2021.

He, B., Chen, C., Lin, S.R., Yuan, W.P., Chen, H.W., Chen, D.L., Zhang, Y.F., Guo, L.L., Zhao, X., Liu, X.B., Piao, S.L., Zhong, Z.Q., Wang, R., Tang, R.: Worldwide impacts of atmospheric vapor pressure deficit on the interannual variability of terrestrial carbon sinks, Natl. Sci. Rev, 9, nwab150, https://doi.org/10.1093/nsr/nwab150, 2022.

Hoffmann, W.A.: Seasonal flooding shapes forest–savanna transitions, PNAS, 120, e2312279120,

https://doi.org/10.5194/egusphere-2024-1226
Preprint. Discussion started: 1 July 2024

https://doi.org/10.1073/pnas.2312279120, 2023.

He, G.X., Shi, Z.T., Fang, H.D., Shi, L.T., Wang, Y.D., Yang, H.Z., Yan, B.G., Yang, C.L., Yu, J.L., Liang, Q.L., Zhao, L., Jiang, Q.: Climate and soil stressed elevation patterns of plant species to determine the aboveground biomass distributions in a valley-type Savanna, Front. Plant Sci, 15, 1324841, https://doi.org/10.3389/fpls.2024.1324841, 2024.

Jin, Z.Z., Ou, X.K., Zhou, Y.: The general situation of natural vegetation in dry-hot river valley of Yuanmou, Yunnan Province, Chin. J. Plant Ecol, 11, 308−317, 1987.

Jiang, J.M., Fei, S.M., He, Y.P., Zhang, F., Kong, Q.H.: Study on vegetation restoration in dry-hot valleys of the Jinsha River, J. Southwest For. Univ, 27, 11–15, https://doi.org/10.11929/j.issn.2095-1914.2007.06.003, 2007.

Jin, Y.Q., Li, J., Liu, C.G., Liu, Y.T., Zhang, Y.P., Song, Q.H., Sha, L.Q., Chen, A.G., Yang, D.X., Li, P.G.: Response of net primary productivity to precipitation exclusion in a savanna ecosystem, For. Ecol. Manage, 29, 69−76, https://doi.org/10.1016/j.foreco.2018.07.007, 2018.

Jin, Y.Q., Li, J., Liu, C.G., Liu, Y.T., Zhang, Y.P., Song, Q.H., Sha, L.Q., Balasubramanian, D., Chen, A.G., Yang, D.X., Li, P.G.: Precipitation reduction alters herbaceous community structure and composition in a savanna, J. Veg. Sci, 30, 821–831, https://doi.org/10.1111/jvs.12766, 2019.

Johnston, A.S.A., Meade, A., Ardö, J., Arriga, N., Black, A., Blanken, P.D., Bonalo, D., Brümmer, C., Cescatti, A., Dušeko, J., Grafo, A., Gioli, B., Godedo, I., Gougho, C.M., Ikawa, H., Jassalo, R., Kobayashi, H., Magliulo, V., Mancao, G., Montagnani, L., Moyano, F.E., Olesen, J.E., Sachs, T., Shao, C.L., Tagesson, T., Wohlfahrt, G., Wolfo, S., Woodgate, W., Varlagin, A., Venditti, C.: Temperature thresholds of ecosystem respiration at a global scale, Nat. Ecol. Evol, 5, 487–494, https://doi.org/10.1038/s41559-021-01398-z, 2021.

Knapp, A., Fay, P.A., Blair, J.M., Collins, S., Smith, M.D., Carlisle, J.D., Harpper, C.W., Danner, B.T., Lett, M.S., Mccarron, J.: Rainfall variability, carbon cycling, and plant species diversity in a mesic grassland, Science, 298, 2202−2205, https://doi.org/10.1126/science.1076347, 2002.

Kato, T., Tang, Y.H., Gu, S., Hirota, M., Du, M.Y., Li, Y.N., Zhao, X.Q.: Temperature and biomass influences on interannual changes in CO_2 exchange in an alpine meadow on the Qinghai-Tibetan Plateau, Global Change Biol, 12, 1285−1298, https://doi.org/10.1111/j.1365-2486.2006.01153.x, 2006.

Kannenberg, S.A., Anderegg, W.R.L., Barnes, M.L., Dannenberg, M.P., Knapp, A.K.: Dominant role of soil moisture in mediating carbon and water fluxes in dryland ecosystems, Nat. Geosci, 17, 38–43, https://doi.org/10.1038/s41561-023-01351-8, 2024.

Law, B.E., Falge, E., Gu, L., Baldocchi, D.D., Bakwin, P., Berbigier, P., Davis, K., Dolman, A.J., Falk, M., Fuentes, J.D., Goldstein, A., Granier, A., Grelle, A., Hollinger, D., Janssens, I.A., Jarvis, P., Jensen, N.O., Katul, G., Mahli, K., Matteucci, G., Meyers, T., Monson, R., Munger, W., Oechel, W., Olson, R., Pilegaard, K., Paw U, K. T., Thorgeirsson, H., Valentini, R., Verma, Shashi., Vesala, T., Wilson, K., Wofsy, S.: Environmental controls over carbon dioxide and water vapor exchange of terrestrial vegetation, Agric. For. Meteorol, 113, 97–120, https://doi.org/10.1016/S0168-1923(02)00104-1, 2002.

Li, S.G., Asanuma, J., Eugster, W., Kotani, A., Liu, J.J., Urano, T., Oikawa, T., Davaa, G., Oyunbaatar, D., Sugita, M.: Net ecosystem carbon dioxide exchange over grazed steppe in central Mongolia, Global Change Biol, 11, 1941–1955, https://doi.org/10.1111/j.1365-2486.2005.01047.x, 2005.

Livesley, S. J., Grover, S., Hutley, L.B., Jamali, H., Butterbach-Bahl, K., Fest, B., Arndt, S. K.:

https://doi.org/10.5194/egusphere-2024-1226
Preprint. Discussion started: 1 July 2024

Seasonal variation and fire effects on CH_4, N_2O and CO_2 exchange in savanna soils of northern Australia, Agric. For. Meteorol, 151, 1440–1452, https://doi.org/10.1016/j.agrformet.2011.02.001, 2011.

Li, J.X., Zeng, H., Zhu, J.T., Zhang, Y.J., Chen, N., Liu, Y.J.: Responses of different experimental warming on ecosystem respiration in Tibetan alpine meadow, Ecol. Environ. Sci, 25, 1612–1620, https://doi.org/10.16258/j.cnki.1674-5906.2016.10.004, 2016.

Li, G.Y., Han, H.Y., Du, Y., Hui, D.F., Xia, J.Y., Niu, S.L., Li, X.N., Wan, S.Q.: Effects of warming and increased precipitation on net ecosystem productivity: a long-term manipulative experiment in a semiarid grassland, Agric. For. Meteorol, 232, 359−366, http://dx.doi.org/10.1016/j.agrformet.2016.09.004, 2017.

Liu, D., Li, Y., Wang, T., Peylin, P., MacBean, N., Ciais, P., Jia, G., Ma, M.G., Ma, Y.M., Shen, M.G., Zhang, X.Z., Piao, S.L.: Contrasting responses of grassland water and carbon exchanges to climate change between Tibetan Plateau and InnerMongolia, Agric. For. Meteorol, 249, 163–175, https://doi.org/10.1016/j.agrformet. 2017.11.034, 2018.

Lee, E., Kumar, P., Barron-Gafford, G.A., Hendryx, S.M., Sanchez-Cañete, E.P., Minor, R.L., Colella, T., Scott, R.L.: Impact of hydraulic redistribution on multispecies vegetation water use in a semiarid savanna ecosystem: an experimental and modeling synthesis, Water Resour. Res, 54, 4009–4027, https://doi.org/10.1029/2017WR021006, 2018.

Liu, J.X., Wang, Z., Duan, Y.F., Li, X.R., Zhang, M.Y., Liu, H.Y., Xue, P., Gong, H.B., Wang, X., Chen, Y., Geng, Y.N.: Effects of land use patterns on the interannual variations of carbon sinks of terrestrial ecosystems in China, Ecol. Indic, 146, 109914, https://doi.org/10.1016/j.ecolind.2023.109914, 2023.

Liu, Z.G., Chen, Z., Yang, M., Hao, T.X., Yu, G.R., Zhu, X.J., Zhang, W.K., Ma, L.X., Dou, X.J., Lin, Y., Luo, W.X., Han, L., Sun, M.Y., Chen, S.P., Dong, G., Gao, Y.H., Hao, Y.B., Jiang, S.C., Li, Y.N., Li, Y.Z., Liu, S.M., Shi, P.L., Tang, Y.K., Xin, X.P., Zhang, F.W., Zhang, Y.J., Zhao, L., Zhou, L., Zhu, Z.L.: Precipitation consistently promotes, but temperature oppositely drives carbon fluxes in temperate and alpine grasslands in China, Agric. For. Meteorol, 344, 109811, https://doi.org/10.1016/j.agrformet.2023.109811, 2024.

Miranda, A.C., Miranda, H.S., Lloyd, J., Grace, J., Francey, R.J., McIntyre, J.A., Meir, P., Riggan, P., Lockwood, R., Brass, J.: Fluxes of carbon, water and energy over Brazilian cerrado, an analysis using eddy covariance and stable isotopes, Plant Cell Environ, 20, 315–328, https://doi.org/10.1046/j.1365-3040.1997.d01-80.x, 1997.

Malhi, Y., Nobre, A., Grace, J., Kruijt, B., Pereira, M., Culf, A., Scott, S.: Carbon dioxide transfer over a central Amazonian rain forest, J. Geophys. Res, 103, 31593–31612, https://doi.org/10.1029/98JD02647, 1998.

Ma, S.Y., Baldocchi, D.D., Xu, L.K., Hehn, T.: Inter-annual variability in carbon dioxide exchange of an oak/grass savanna and open grassland in California, Agric. For. Meteorol, 147, 157–171. https://doi.org/10.1016/j.agrformet.2007.07.008, 2007.

Millard, P., Midwood, A. J., Hunt, J.E., Whitehead, D., Boutton, T.W.: Partitioning soil surface CO_2 efflux into autotrophic and heterotrophic components, using natural gradients in soil $\delta^{13}C$ in an undisturbed savannah soil, Soil Biol. Biochem, 40, 1575–1582, https://doi.org/10.1016/j.soilbio.2008.01.011, 2008.

McDowell, N.G., Allen, C.D.: Darcy's law predicts widespread forest mortality under climate warming, Nat. Clim. Change, 5, 669–72, https://doi.org/10.1038/nclimate2641, 2015.

https://doi.org/10.5194/egusphere-2024-1226
Preprint. Discussion started: 1 July 2024

Mattos, C.R.C., Hirota, M., Oliveira, R.S., Flores, B.M., Miguez-Macho, G., Pokhrel, Y., Fan, Y.: Double stress of waterlogging and drought drives forest–savanna coexistence, PNAS, 120, e2301255120, https://doi.org/10.1073/pnas.2301255120, 2023.

Niu, S.L., Wu, M.Y., Han, Y., Xia, J.Y., Li, L.H., Wan, S.Q.: Water-mediated responses of ecosystem carbon fluxes to climatic change in a temperate steppe, New Phytol, 177, 209−219, https://doi.org/10.1111/j.1469-8137. 2007.02237.x, 2017.

Novick, K.A., Miniat, C.F., Vose, J.M.: Drought limitations to leaf-level gas exchange: results from a model linking stomatal optimization and cohesion–tension theory, Plant Cell Environ, 39, 583–96, https://doi.org/10.1111/pce.12657, 2016.

Niu, Y.Y., Li, Y.Q., Wang, X.Y., Gong, X.W., Luo, Y.Q., Tian, D.Y.: Characteristics of annual variation in net carbon dioxide flux in a sandy grassland ecosystem during dry years, Acta Prataculturae Sin, 27, 215–221, https://doi.org/10.11686/cyxb2017231, 2018.

Peel, M.C., Finlayson, B.L., McMahon, T.A.: Updated world map of the Köppen-Geiger climate classification, Hydrol. Earth Syst, Sci. 11, 1633–1644, https://doi.org/10.5194/hess-11-1633-2007, 2007.

Piao, S.L., Huang, M.T., Liu, Z., Wang, X.H., Ciais, P., Canadell, J.G., Wang, K., Bastos, A., Friedlingstei, P., Houghto, R.A., Quéré, C.L., Liu, Y.W., Myneni, R.B., Peng, S.S., Pongratz, J., Sitch, S., Yan, T., Wang, Y.L., Zhu, Z.C., Wu, D.H., Wang, T.: Lower land-use emissions responsible for increased net land carbon sink during the slow warming period, Nat. Geosci. 11, 739–743, https://doi.org/10.1038/s41561-018-0204-7, 2018.

Pan, S.F., Yang, J., Tian, H.Q., Shi, H., Chang, J.F., Ciais, P., Francois, L., Frieler, K., Fu, B.J., Hickler, T., Ito, A., Nishina, K., Ostberg, S., Reyer, C.P.O., Schaphoff, S., Steinkamp, J., Zhao, F.: Climate extreme versus carbon extreme: responses of terrestrial carbon fluxes to temperature and precipitation, J. Geophys. Res.: Biogeosci, 125, e2019JG005252, https://doi.org/10.1029/2019JG005252, 2020.

Quansah, E., Mauder, M., Balogun, A.A., Amekudz, L.K., Hingerl, L., Bliefernicht, J., Kunstmann, H.: Carbon dioxide fluxes from contrasting ecosystems in the Sudanian savanna in West Africa, Carbon Balance Manage, 10, 1, https://doi.org/10.1186/s13021-014-0011-4, 2015.

Ruimy, A., Jarvis, P.G., Baldocchi, D.D., Saugier, B.: CO_2 fluxes over plant canopies and solar radiation: a review, Adv. Ecol. Res, 26, 1–68, https://doi.org/10.1016/s0065-2504(08)60063-x, 1995.

Santos, A.J.B., Silva, G.T.D.A., Miranda, H.S., Miranda, A.C., Lloyd, J.: Effects of fire on surface carbon, energy and water vapour fluxes over campo sujo savanna in central Brazil, Funct. Ecol, 17, 711–719, https://doi.org/10.1111/j.1365-2435.2003.00790.x, 2003.

Saleska, S.R., Millar, S.D., Martos, D.M., Goulden, M.L., Wofsy, S.C., da Rocha, H.R., De Camargo, P.B., Crill, P., Daule, B.C., De Freitas, H.C., Hutyra, L., Keller, M., Kirchhoff, V., Menton, M., Munger, J.W., Pyle, E.H., Rice, A.H., Silva, H.: Carbon in Amazon forests: unexpected seasonal fluxes and disturbance-induced losses, Science, 302, 1554–1557, https://doi.org/10.1126/science.1091165, 2003.

Serrano-Ortiz, P., Domingo, F., Cazorla, A., Were, A., Cuezva, S., Villagarcía, L., Alados-Arboledas, L., Kowalski, A.S.: Interannual CO_2 exchange of a sparse mediterranean shrubland on a carbonaceous substrate, J. Geophys. Res.: Biogeosci, 114, https://doi.org/Artn G0401510.1029/2009jg000983, 2009.

Shen, R., Zhang, J.L., He, B., Li, F., Zhang, Z.M., Zhou, R., Ou, X.K.: The structure characteristic

and analysis on similarity of grassland community in dry-hot valley of Yuanjiang, Ecol. Environ. Sci, 19, 2821–2825, https://doi.org/10.16258/j.cnki.1674-5906.2010.12.011, 2010.
Sulman, B.N., Roman, D.T., Yi, K., Wang, L.X., Phillips, R.P., Novick, K.A.: High atmospheric demand for water can limit forest carbon uptake and transpiration as severely as dry soil, Geophys. Res. Lett, 43, 9686–95, https://doi.org/10.1002/2016GL069416, 2016.
Sun, S.S., Wu, Z.P., Xiao, Q.T., Yu, F., Gu, S.H., Fang, D., Li, L., Zhao, X.B.: Factors influencing CO_2, fluxes of a grassland ecosystem on the Yunnan-Guizhou Plateau, China, Acta Prataculturae Sin, 29, 184–191, https://doi.org/10.7522/.10.11686/cyxb2019410, 2020.
Sha, Z.Y., Bai, Y.F., Li, R.R., Lan, H., Zhang, X.L., Li, J., Liu, X.F., Chang, S.J., Xie, Y.C.: The global carbon sink potential of terrestrial vegetation can be increased substantially by optimal land management, Commun. Earth Environ, 3, 8, https://doi. 10.1038/s43247-021-00333-1, 2022.
Tagesson, T., Fensholt, R., Cropley, F., Guiro, I., Horion., S. Ehammer. A., Ardö., J.: Dynamics in carbon exchange fluxes for a grazed semi-arid savanna ecosystem in West Africa, Agric. Ecosyst. Environ, 205, 15–24, https://doi.org/ 10.1016/j.agee.2015.02.017, 2015.
Tarin, T., Nolan, R.H., Eamus, D., Cleverly, J.: Carbon and water fluxes in two adjacent Australian semi-arid ecosystems, Agric. For. Meteorol, 281, 107853, https://doi.org/10.1016/j.agrformet.2019.107853, 2020.
Veenendaal, E.M., Kolle, O., Lloyd, J.: Seasonal variation in energy fluxes and carbon dioxide exchange for a broad-leaved semiarid savanna (Mopane woodland) in Southern Africa, Global Change Biol, 10, 318–328, https://doi.org/10.1111/j.1365-2486.2003.00699.x, 2004.
Woodwell, G.M., Hobbie, J.E., Houghton, R.A., Melillo, J.M., Mooer, B., Peterson, B.J., Shaver, G.R.: Global deforestation: contribution to atmospheric carbon dioxide, Science, 222, 1081–1086, https://doi.org/10.1126/science.222.4628.1081, 1983.
White, R.P., Murray, S., Rohweder, M.: Pilot analysis of global ecosystems: grassland ecosystems, World Resources Institute, Washington, DC, http://www. wri.org/wr2000, 2000.
Weltzin, J.F., Loik, M.E., Schwinning, S., Williams, D.G., Fay, P.A., Haddad, B.M., Harte, J., Huxman, T.E., Knapp, A.K., Lin, G.H., Pockman, W.T., Shaw, R.M., Small, E.E., Smith, M.D., Smith, S.D., Tissue, D.T., Zak, J.C.: Assessing the response of terrestrial ecosystems to potential changes in precipitation, BioScience, 53, 941–952, https://doi.org/10.1641/0006-3568(2003)053[0941:ATROTE]2.0.CO;2, 2003.
Wen, X.F., Sun, X.M., Liu, Y.F., Li, X.B.: Effect of linear and exponential fitting on the initial rate of change in CO_2 concentration across the soil surface, Chin. J. Plant Ecol, 31, 380–385, https://doi.org/10.17521/cjpe.2007.0046, 2007.
Williams, A.P., Allen, C.D., Macalady, A.K., Griffin, D., Woodhouse, C.A., Meko, D.M., Swetnam, T.W., Rauscher, S.A., Seager, R., Grissino-Mayer, H.D., Dean, J.S., Cook, E.R., Gangodagamage, C., Cai, M., McDowell, N.G.: Temperature as a potent driver of regional forest drought stress and tree mortality, Nat. Clim. Change, 3, 292–297, https://doi.org/10.1038/nclimate1693, 2013.
Wang, W.Y., Guo, J.X., Wang, Y.S., Wu, K.: Observing characteristics of CO_2 flux and its influencing factors over Xilinhot grassland, J. Meteorol. Sci, 35, 100–107, https://doi.org/10. 3969 /2013jms. 0065, 2015.
Wu, F.T., Cao, S.K., Cao, G.C., Han, G.Z., Lin, Y.Y., Cheng, S.Y.: Variation of CO_2 flux of alpine wetland ecosystem of *Kobresta tibetica* wet meadow in Lake Qinghai, J. Ecol. Rural Environ,

34, 124–131, https://doi.org/10.11934/1.19n.1673-4831.2018.02.004, 2018.

Wang, N., Quesada, B., Xia, L.L., Butterbach-Bahl, K., Goodale, C.L., Kiese, R.: Effects of climate warming on carbon fluxes in grasslands – a global meta-analysis, Global Change Biol, 25, 1839–1851, https://doi.org/10.1111/gcb.14603, 2019.

Wang, Y.Y., Xiao, J.F., Ma, Y.M., Luo, Y.Q., Hu, Z.Y., Li, F., Li Y.N., Gu, L.L., Li, Z.G., Yuan, L.: Carbon fluxes and environmental controls across different alpine grassland types on the Tibetan Plateau, Agric. For. Meteorol, 311, 1–14, https://doi.org/10.1016/j.agrformet.2021.108694, 2021.

Wang, H.H., Huang, W.D., He, Y.Z., Zhu, Y.Z.: Effects of warming and precipitation reduction on soil respiration in Horqin sandy grassland, northern China, Catena, 233, 107470, https://doi.org/10.1016/j.catena.2023.107470, 2023.

Wang, F., Harindintwali, J.D., Wei, K., Shan, Y.L., Mi, Z.F., Costello, M.J., Grunwald, S., Feng, Z.Z., Wang, F.M., Guo, Y.M., Wu, X., Kumar, P., Kästner, M., Feng, X.J., Kang, S.C., Liu, Z., Fu, Y.H., Zhao, W., Ouyang, C.J., Shen, J.L., Wang, H.J., Chang, S.X., Evans, D.L., Wang, R., Zhu, C.W., Xiang, L.L., Rinklebe, J., Du, M.M., Huang, L., Bai, Z.H., Li, S., Lal, R., Elsner, M., Wigneron, J.P., Florindo, F., Jiang, X., Shaheen, S.M., Zhong, X.Y., Bol, R., Vasques, G.M., Li, X.F., Pfautsch, S., Wang, M.G., He, X., Agathokleous, E., Du, H.B., Kengara, F.O., Brahushi, F., Long, X.E., Pereira, P., Ok, Y.S., Rillig, M.C., Jeppesen, E., Barceló, D., Yan, X.Y., Jiao, N.Z., Han, B.X., Schäffer, A., Chen, J.M., Zhu, Y.G., Cheng, H., Amelung, W., Spötl, C., Zhu, J.K., Tiedje, J.M.: Climate change: Strategies for mitigation and adaptation, The Innovation Geosci, 1, 100015, https://doi. 10.59717/j.xinn-geo.2023.100015, 2023.

Xu, X.L: China watershed and river network datasets based on DEM extraction, Resource and Environmental Science Data Registration and Publishing System [data set], https://doi.org/10.12078/2018060101, 2018.

Xu, X.L: China's multi-year provincial administrative division boundary data, Resource and Environmental Science Data Registration and Publishing System [data set], https://doi.org/10.12078/2023010103, 2023a.

Xu, X.L: China's multi-year county administrative division boundary data, Resource and Environmental Science Data Registration and Publishing System [data set], https://doi.org/10.12078/2023010101, 2023b.

Xu, Y.N., Wang, X., Sun, Y.R., Liu, H.T., Li, L., Schäufele, R., Gong, X.Y.: Response of photosynthetic ^{13}C discrimination to vapour pressure deficit reflects changes in bundle-sheath leakiness in two C_4 grasses, Environ. Exp. Bot, 216, 105529, https://doi.org/10.1016/j.envexpbot.2023.105529, 2023.

Yu, K., D'Odorico, P.: Hydraulic lift as a determinant of tree–grass coexistence on savannas, New Phytol, 207, 1038–1051, https://doi.org/10.1111/nph.13431, 2015.

Yuan, W.P., Zheng, Y., Piao, S.L., Ciais, P., Lombardozzi, D., Wang, Y.P., Ryu, Y., Chen, G.X., Dong, W.J., Hu, Z.M., Jain, A.K., Jiang, C.Y., Kato, E., Li, S.H., Lienert, S., Liu, S.G., Nabel, J.E.M.S., Qin, Z.C., Quine, T., Sitch, S., Smith, W.K., Wang, F., Wu, C.Y., Xiao, Z.Q., Yang, S.: Increased atmospheric vapor pressure deficit reduces global vegetation growth, Sci. Adv, 5, eaax1396, https://doi.org/10.1126/sciadv.aax1396, 2019.

Yang, K.Y., Gong, H.D., Li, J., Liu, Y.T., Sha, L.Q., Song, Q.H., Jin, Y.Q., Yang, D.X., Li, P.G., Wen, G.J., Chen, A.G., Pang, Z.Q., Zhang, Y.P.: Dynamic characteristics of soil respiration of savanna ecosystem in dry hot valley of Yuanjiang, J. Zhejiang Agric. For. Univ, 37, 849–859,

https://doi.org/10.5194/egusphere-2024-1226
Preprint. Discussion started: 1 July 2024

https://doi.org/10.11833/j.issn.2095-0756.20190647, 2020.

Yang, Y.H., Shi, Y., Sun, W.J., Chang, J.F., Zhu, J.X., Chen, L.Y., Wang, X., Guo, Y.P., Hongtu, Z., Yu, L.F., Zhao, S.Q., Xu, K., Zhu, J.L., Shen, H.H., Wang, Y.Y., Peng, Y.F., Zhao, X., Wang, X.Q., Hu, H.F., Chen, S.Q., Huang, M., Wen, X.F., Wang, S.P., Zhu, B., Niu, S.L., Tang, Z.Y., Liu, L.L., Fang, J.Y.: Terrestrial carbon sinks in China and around the world and their contribution to carbon neutrality, Sci. China Life Sci, 65, 861–895, https://doi.org/10.1007/s11427-021-2045-5, 2022.

Zhang, R.Z.: The dry valley of the Henduan Mountains region, Beijing Sci. Press, ISBN 703002916X, 1992.

Zhao, L., Gu, S., Xu, S.X., Zhao, X.Q., Li, Y.N.: Carbon flux and controlling process of alpine meadow on Qinghai-Tibetan plateau, Acta Botan. Boreali-Occidentalia Sin, 27, 1054–1060, 2007.

Zhang F.W., Li, Y.N., Cao, G.M., Li, F.X., Ye, G.J., Liu, J.H., Wei, Y.L., Zhao, X.Q.: CO_2 fluxes and their driving factors over alpine meadow grassland ecosystems in the northern shore of Qinghai Lake, China, Chin. J. Plant Ecol, 36,187–198, https://doi.org/10.3724/SP.J.1258.2012.00187, 2012.

Zou, H., Gao, G.Y., Fu, B.J.: The relationship between grassland ecosystem and soil water in arid and semi-arid areas: a review, Acta Ecol. Sin, 36, 3127–3136, https://doi.org/10.5846/stxb201506211251, 2016.

Zhang, W.M., Brandt, M., Penuelas, J., Guichard, F., Tong, X., Tian, F., Fensholt, R.: Ecosystem structural changes controlled by altered rainfall climatology in tropical savannas, Nat. Commun, 10, 671, https://doi.org/10.1038/s41467-019-08602-6, 2019.

Zhang, R., Zhao, X.Y., Zuo, X.A., Qu, H., Degen, A.A., Luo, Y.Y., Ma, X.J., Chen, M., Liu, L.X., Chen, J.L.: Impacts of precipitation on ecosystem carbon fluxes in desert-grasslands in Inner Mongolia, China, J. Geophys. Res. Atmos, 124, 1266–1276, https://doi.org/10.1029/2018JD028419, 2019.

Zhao, H.C., Jia, G.S., Wang, H.S., Zhang, A.Z., Xu, X.Y.: Diurnal variations of the carbon fluxes of semiarid meadow steppe and typical steppe in China, Clim. Environ. Res, 25, 172–184, https://doi.org/10.3878/j.issn.1006-9585.2019.19096, 2020.

Zhang, Y.J., Qiu, L.P., Gao, H.L., Liu. J., Wei, X.R., Zhang, X.C.: Responses of ecosystem CO_2 exchange to clipping in a semi-arid typical grassland on the Loess Plateau, Acta Ecol. Sin, 40, 336–344, https://doi.org/10.5846/stxb201810172244, 2020.

Zeng, Z.Q., Wu, W.X., Li, Y.M., Huang, C., Zhang, X.Q., Peñuelas, J., Zhang, Y., Gentine, P., Li, Z.L., Wang, X.Y., Huang, H., Ren, X.S., Ge, Q.S.: Increasing meteorological drought under climate change reduces terrestrial ecosystem productivity and carbon storage, One Earth, 6, 1326–1339, https://doi.org/10.1016/j.oneear.2023.09.007, 2023.

Zhou, Y., Bomfim, B., Bond, W.J., Boutton, T.W., Case, M.F., Coetsee, C., Davies, A.B., February, E.C., Gray, E.F., Silva, L.C.R., Wrigh, J., Staver, A.C.: Soil carbon in tropical savannas mostly derived from grasses, Nat. Geosci, 16, 710–716, https://www.nature.com/articles/s41561-023-01232-0, 2023.

Zhong, Z.Q., He, B., Wang, Y.P., Chen, H.W., Chen, D.L., Fu, Y.S.H., Chen, Y.N., Guo, L.L., Deng, Y., Huang, L., Yuan, W.P., Hao, X.M., Tang, R., Liu, H.M., Sun, L.Y., Xie, X.M., Zhang, Y.F.: Disentangling the effects of vapor pressure deficit on northern terrestrial vegetation productivity, Sci. Adv, 9, eadf3166, https://doi.org/10.1126/sciadv.adf3166, 2023.